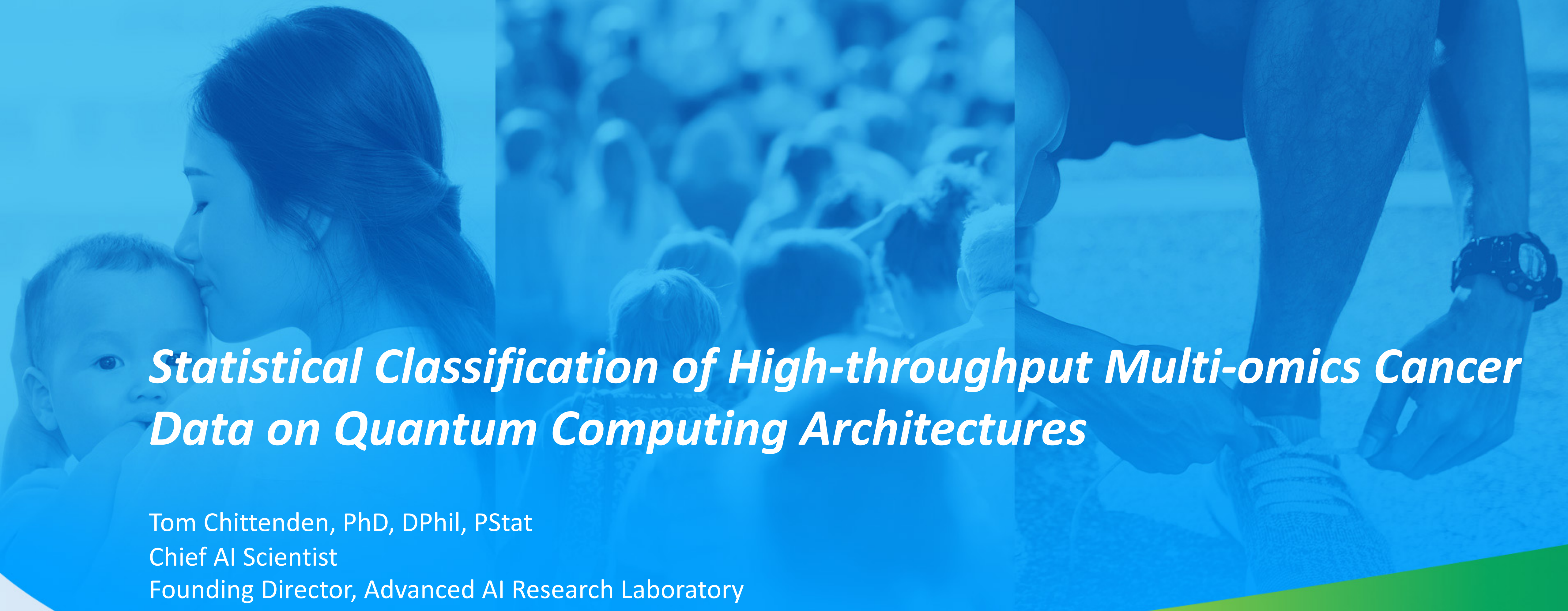

Statistical Classification of High-throughput Multi-omics Cancer Data on Quantum Computing Architectures

Tom Chittenden, PhD, DPhil, PStat
Chief AI Scientist
Founding Director, Advanced AI Research Laboratory
Lecturer on Pediatrics, Harvard Medical School

WuXiNextCODE

WuXi NextCODE Global Predictive Analytics Initiative

deepCODE Deep Learning and Probabilistic Programming – Faster, cost-effective drug development

Adding value to drug discovery pipelines

- **Drug target discovery and drug repurposing with novel ensemble computational intelligence strategies with integrated data platforms to identify 'causal' driver genes and molecular signaling transduction networks**
  - ***Proof of concept for causal statistical learning approaches.***
  - ***Focus of Today's Talk.***
- **Discover accurate integrated 'omics' profile that defines responders and non-responders for a drug in development**
  - ***Pharma partners can use our profile to decrease cost and time of phase II or phase III trials.***
  - ***WXNC can provide sequencing/ GOR database/ analysis/ deep learning.***
  - ***Note approach may work on small sample sizes - deep learning is powerful enough to potentially find drug response profiles even in phase I clinical trials with only 40 to 60 patients on drug.***
- **Discover accurate integrated 'omics' profile that defines responders and non-responders for an approved expensive drug that is being underutilized**
  - ***Pharma can use our profile to justify use and reimbursement for their drug.***
  - ***A drug response profile could salvage the marketing of their drug.***

AI & Deep Learning

Facial Recognition & DeepCODE Feature Selection Analogy

(Facebook AI team's Facial Recognition Algorithm boasts 97.25% Accuracy)

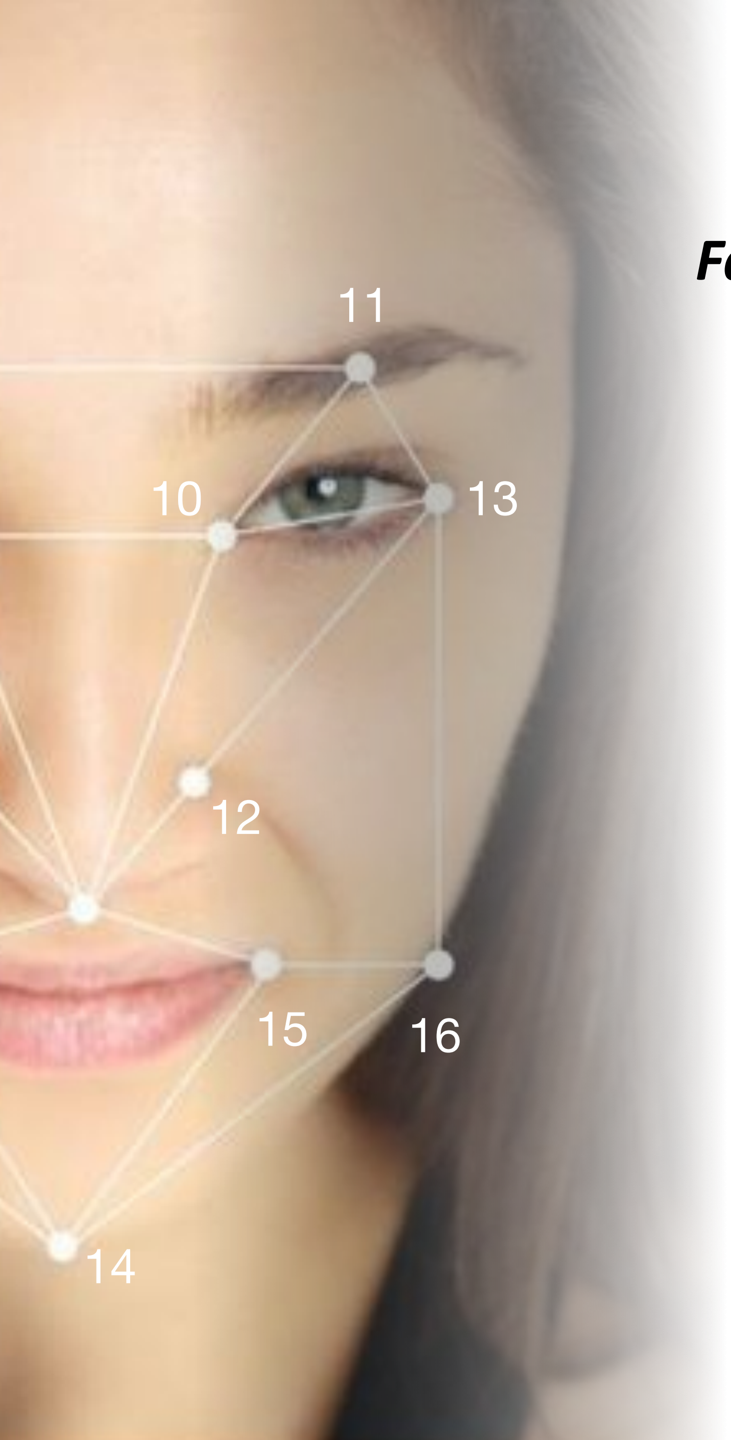

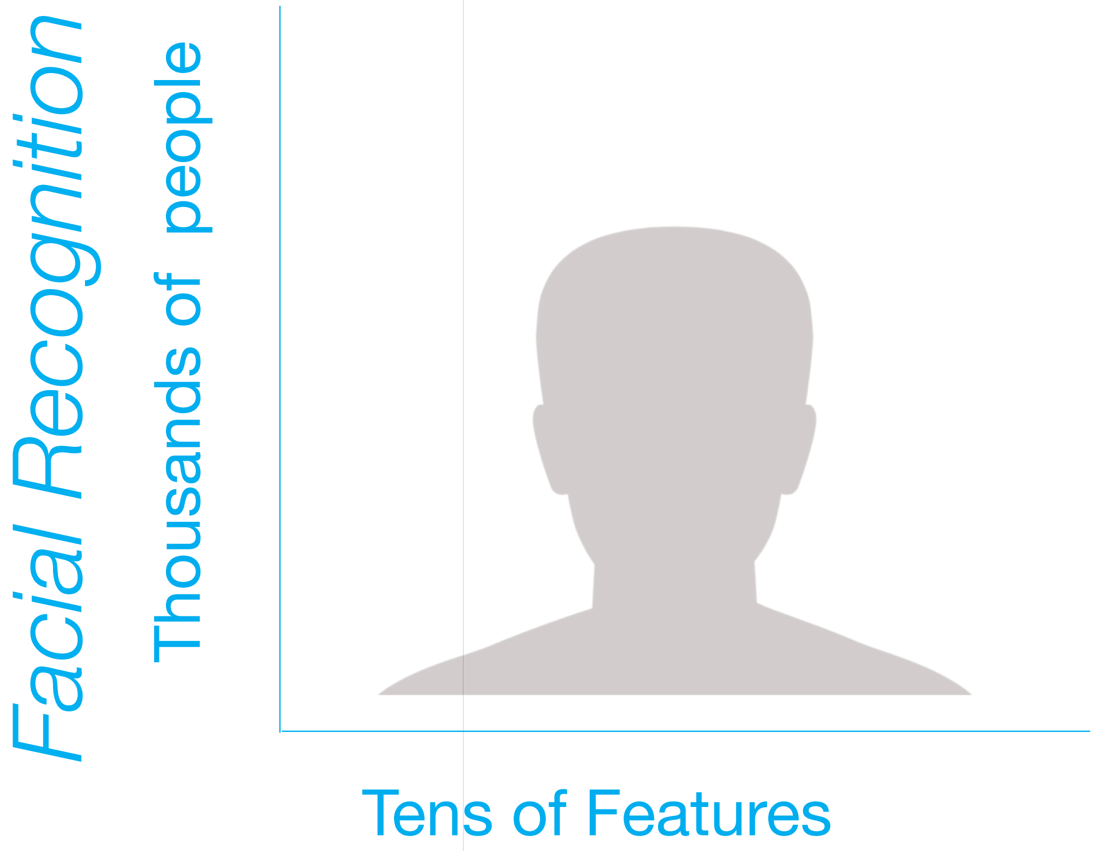

Our deepCODE dimensionality reduction methods enhance algorithm stability and allow us to handle tens of thousands of features without overfitting

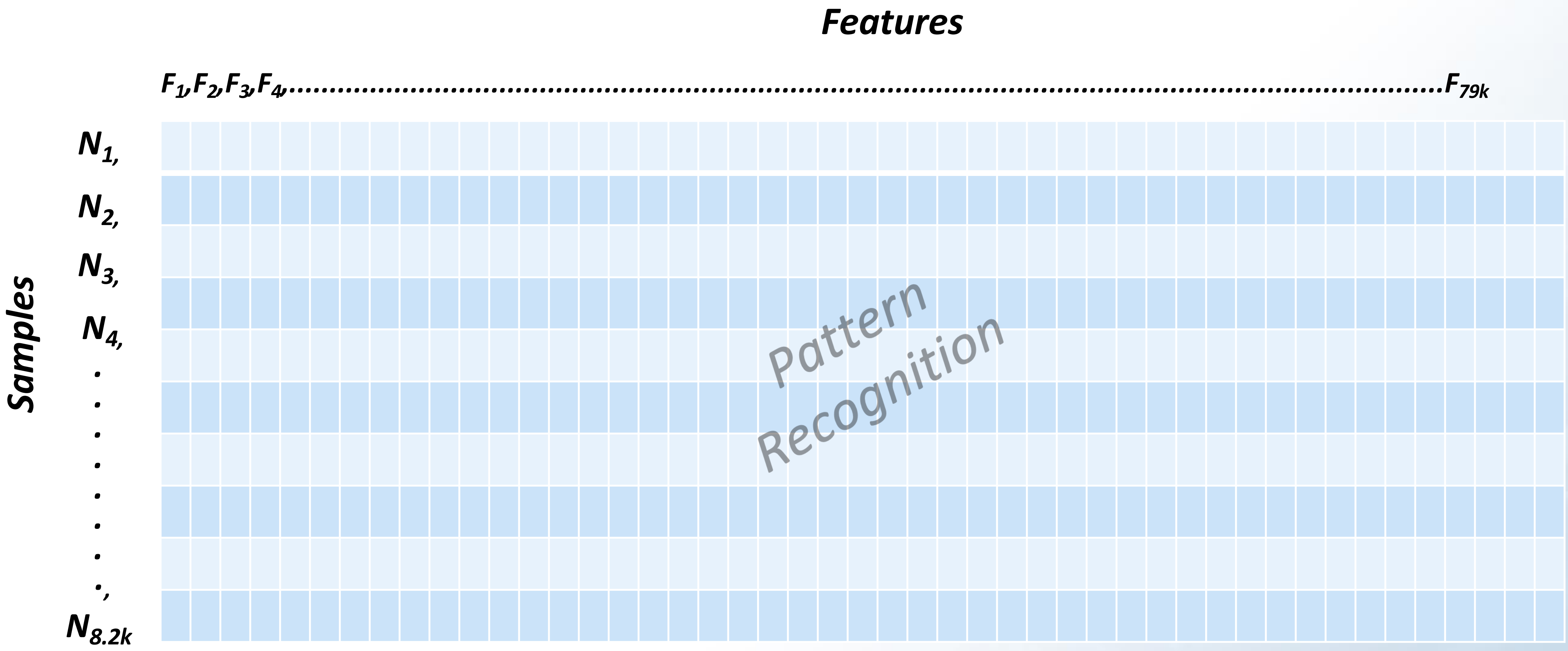

Features

F_1,F_2,F_3,F_4,..F_{79k}

Samples

$N_{1,}$

$N_{2,}$

$N_{3,}$

$N_{4,}$

.

.

.

.

.

.

.

.,

$N_{8.2k}$

Pattern Recognition

A.I. and Precision Medicine

The computational power of modern A.I. technology is well-positioned to uncover new and actionable insights from the exponentially growing pool of biological data.

FEATURE LEARNING

The intelligent simplification of high-dimensional multi-omic data without loss of information

MACHINE & DEEP LEARNING

Intelligent algorithms capable of self-optimization to achieve incredible accuracy with complex, layered data

CAUSAL INFERENCE

Specialized statistical learning models capable of elucidating casual dependencies within biological data

NATURAL LANGUAGE PROCESSING

Intelligent scanning of sentence syntax to understand and validate findings in context, at scale

The combination of several A.I. methods create a proprietary ensemble A.I. strategy capable of revealing novel patterns and causal dependencies in disparate and varied biological data.

Ensemble Computational Intelligence

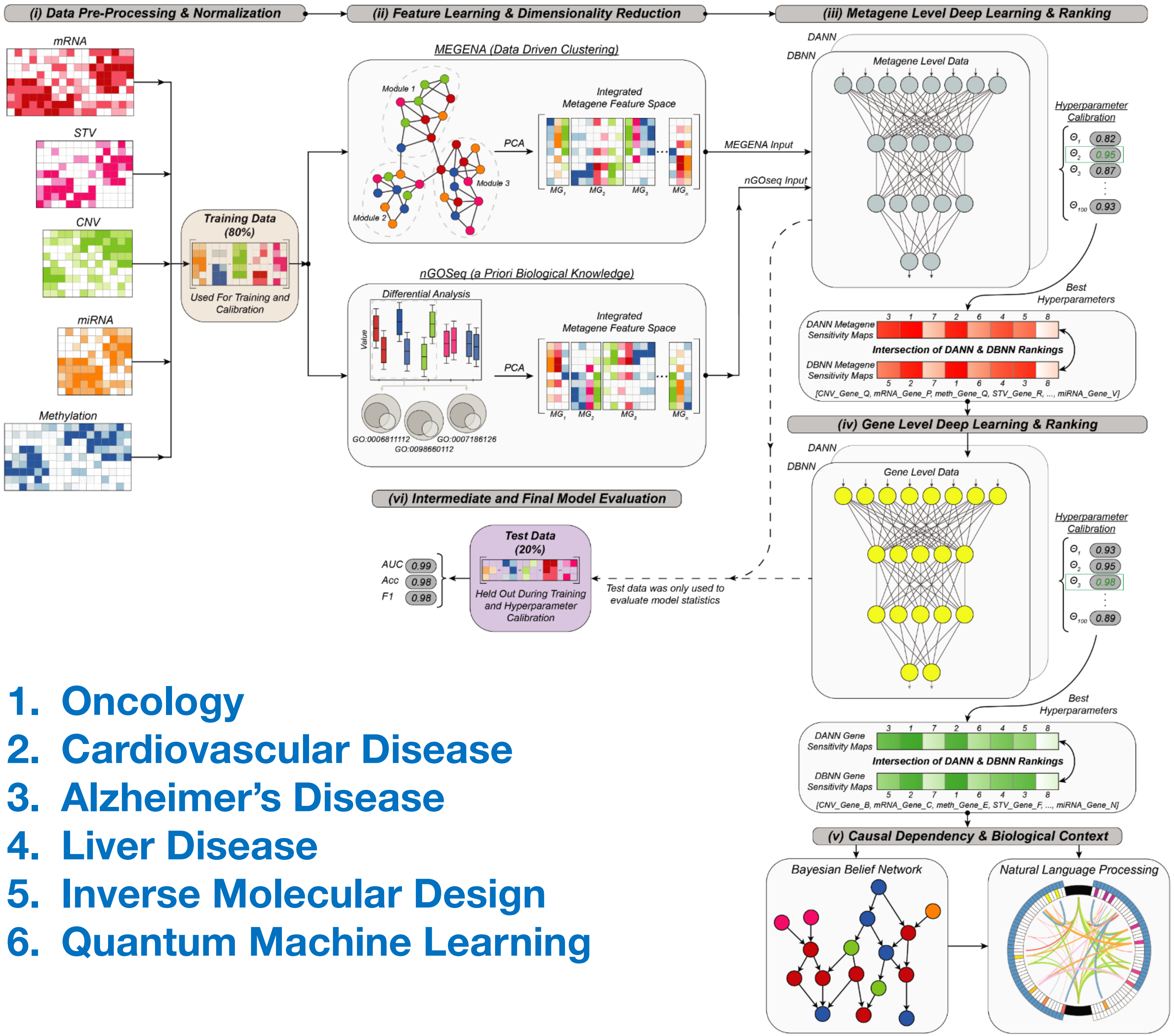

(i) Data Pre-Processing & Normalization
(ii) Feature Learning & Dimensionality Reduction
(iii) Metagene Level Deep Learning & Ranking
mRNA
STV
CNV
miRNA
Methylation
Training Data (80%)
Used For Training and Calibration
MEGENA (Data Driven Clustering)
Module 1
Module 2
Module 3
PCA
Integrated Metagene Feature Space
MG1
MG2
MG3
MGn
nGOSeq (a Priori Biological Knowledge)
Differential Analysis
Value
GO:0006811112
GO:0098660112
GO:0007186126
MEGENA Input
nGOseq Input
DANN
DBNN
Metagene Level Data
Hyperparameter Calibration
Θ1 0.82
Θ2 0.95
Θ3 0.87
Θ100 0.93
Best Hyperparameters
DANN Metagene Sensitivity Maps
Intersection of DANN & DBNN Rankings
DBNN Metagene Sensitivity Maps
3 1 7 2 6 4 5 8
5 2 7 1 6 4 3 8
[CNV_Gene_Q, mRNA_Gene_P, meth_Gene_Q, STV_Gene_R, ..., miRNA_Gene_V]
(iv) Gene Level Deep Learning & Ranking
Gene Level Data
Θ1 0.93
Θ2 0.95
Θ3 0.98
Θ100 0.89
DANN Gene Sensitivity Maps
DBNN Gene Sensitivity Maps
[CNV_Gene_B, mRNA_Gene_C, meth_Gene_E, STV_Gene_F, ..., miRNA_Gene_N]
(vi) Intermediate and Final Model Evaluation
AUC 0.99
Acc 0.98
F1 0.98
Test Data (20%)
Held Out During Training and Hyperparameter Calibration
Test data was only used to evaluate model statistics
(v) Causal Dependency & Biological Context
Bayesian Belief Network
Natural Language Processing

1. **Oncology**
2. **Cardiovascular Disease**
3. **Alzheimer’s Disease**
4. **Liver Disease**
5. **Inverse Molecular Design**
6. **Quantum Machine Learning**

Ensemble Computational Intelligence

Enhanced Feature Reproducibility for Causal Statistical Learning

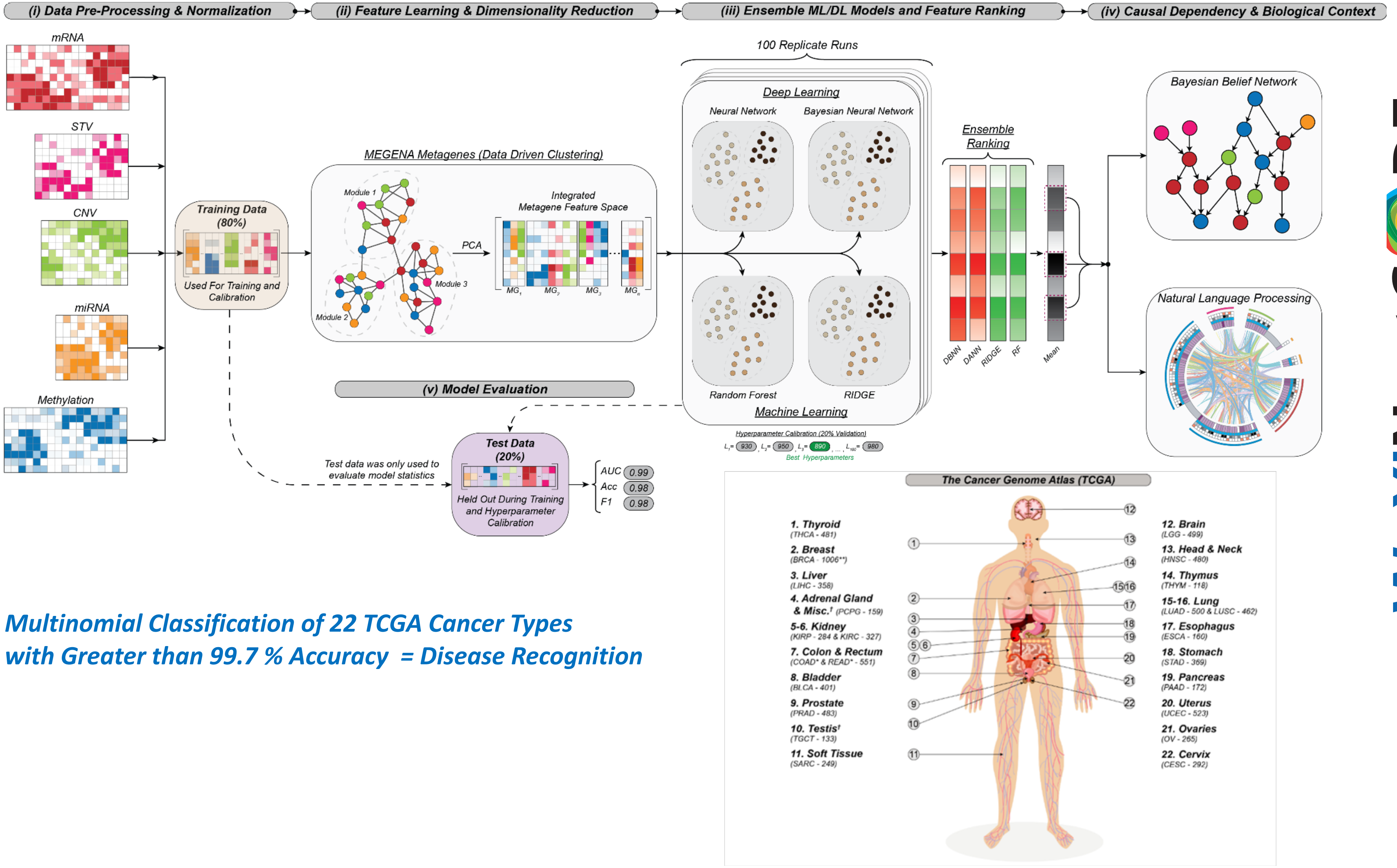

Multinomial Classification of 22 TCGA Cancer Types
with Greater than 99.7 % Accuracy = Disease Recognition

Large-scale clinical outcome study:
TCGA Pan-Cancer Time-dependent Survival Analysis

Prediction of overall survival across 20 different cancers types with 75% accuracy

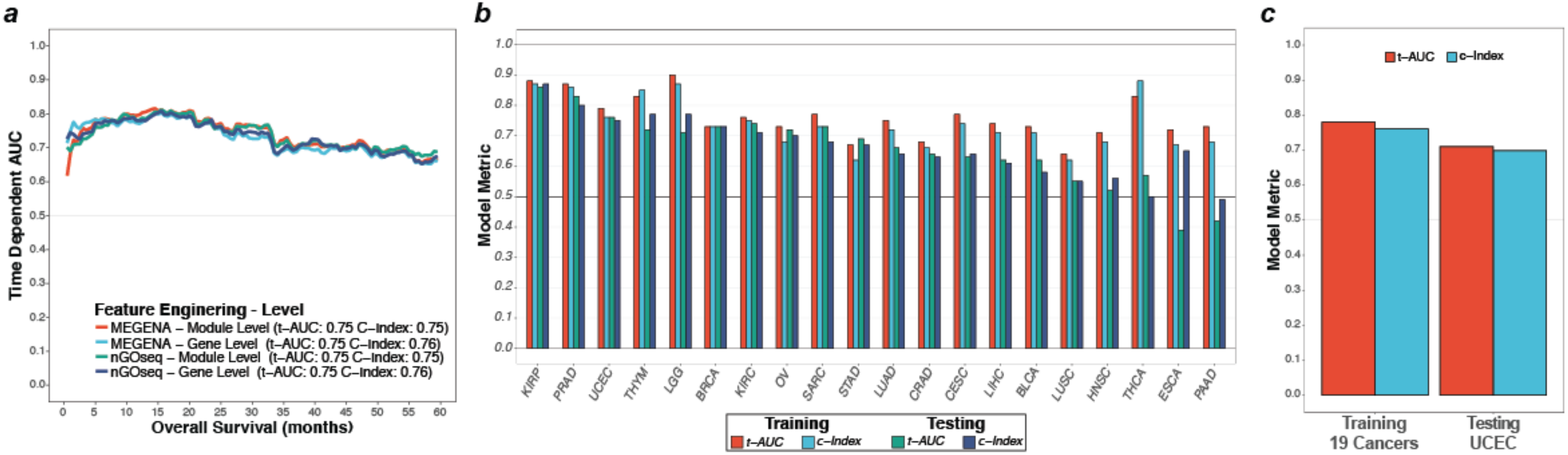

Data Matrix

- 79k Molecular Features + 1 Clinical variable: Age
- 6,122 Training Samples
- 1,853 Testing Samples
- 20 Cancer Types

Interpretation: Compensating for overall survival instead of disease specific survival

Estimator of cumulative/dynamic AUC for right-censored time-to-event data: Uno *et al*. *Journal of the American Statistical Association*, 2007

Large-scale clinical outcome study: TCGA Pan-Cancer Survival Analysis

Risk Stratification across 20 TCGA Cancers Types

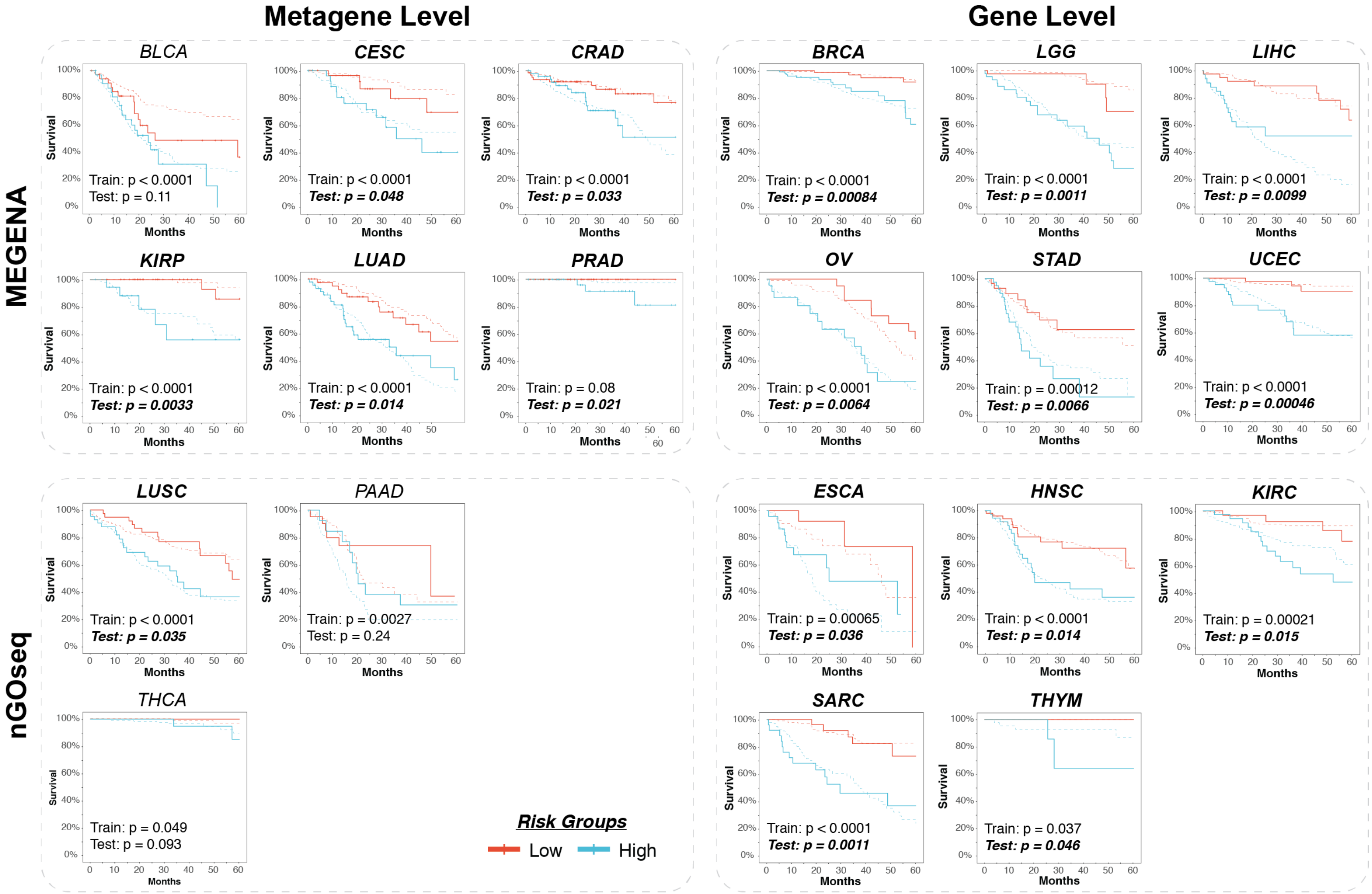

Blue = DNA Methylation
Red = mRNA
Orange = miRNA
Green = CNV
Pink = STV

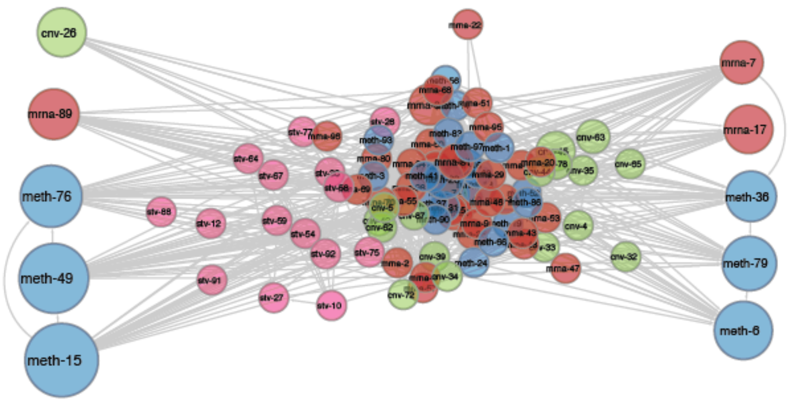

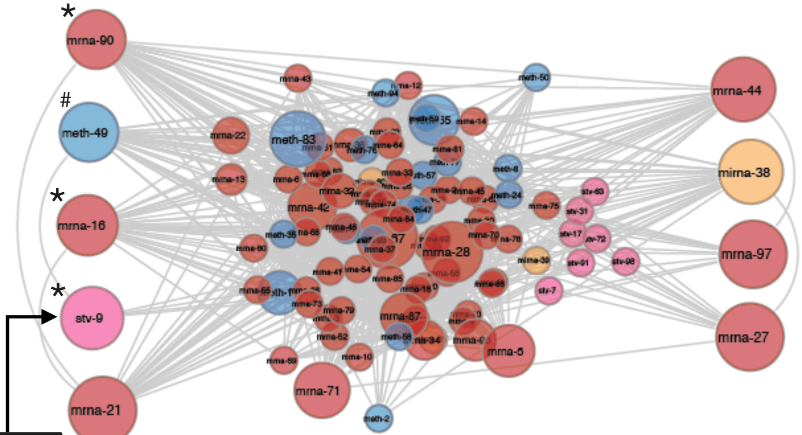

Bayesian Belief Networks

CDK4

Purple Band = Degree NLP Network Connectivity
Black Band = Degree BNN Node Connectivity
Blue Band = Function Annotation
Red = BNN Driver Gene
Bold + Italic = Known Drug Target
*Driver Gene & Known Drug Target
#Driver Gene of Unknown Function

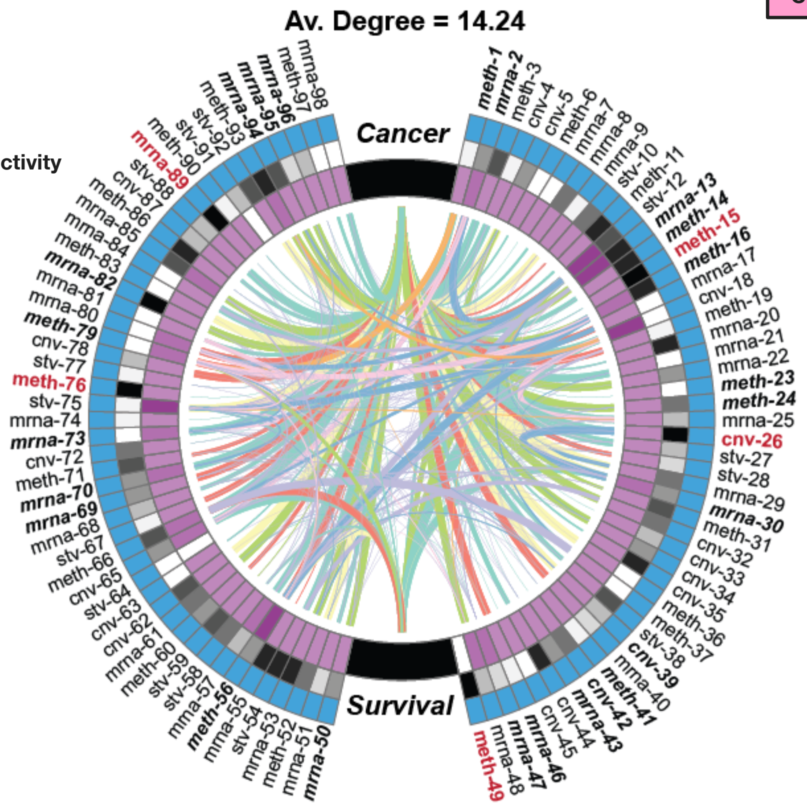

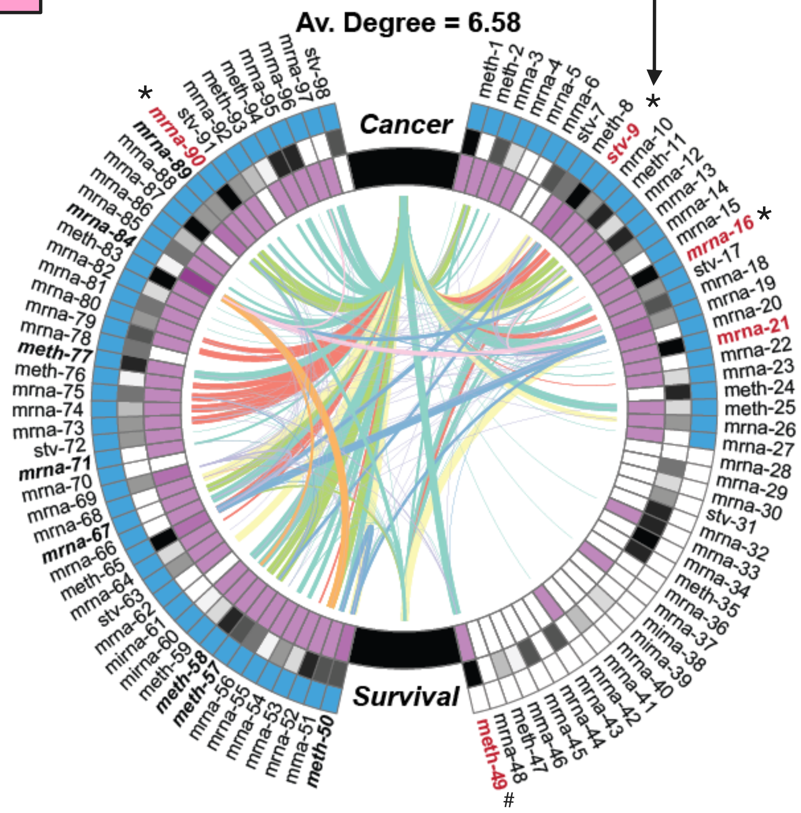

Natural Language Processing

nGOseq
DNA Methylation = 8
mRNA = 14
CNV = 2

MEGENA
DNA Methylation = 3
mRNA = 7
STV = 1

nGOseq

MEGENA

WuXiNextCODE

CDK4 KO confirmation by WB:

***Approved CDK4/6 inhibitors** for metastatic ER-positive/HER2-negative breast cancer: *Kisqali* (Norvartis), *Verzenio* (Lilly), and *Ibrance* (Pfizer).

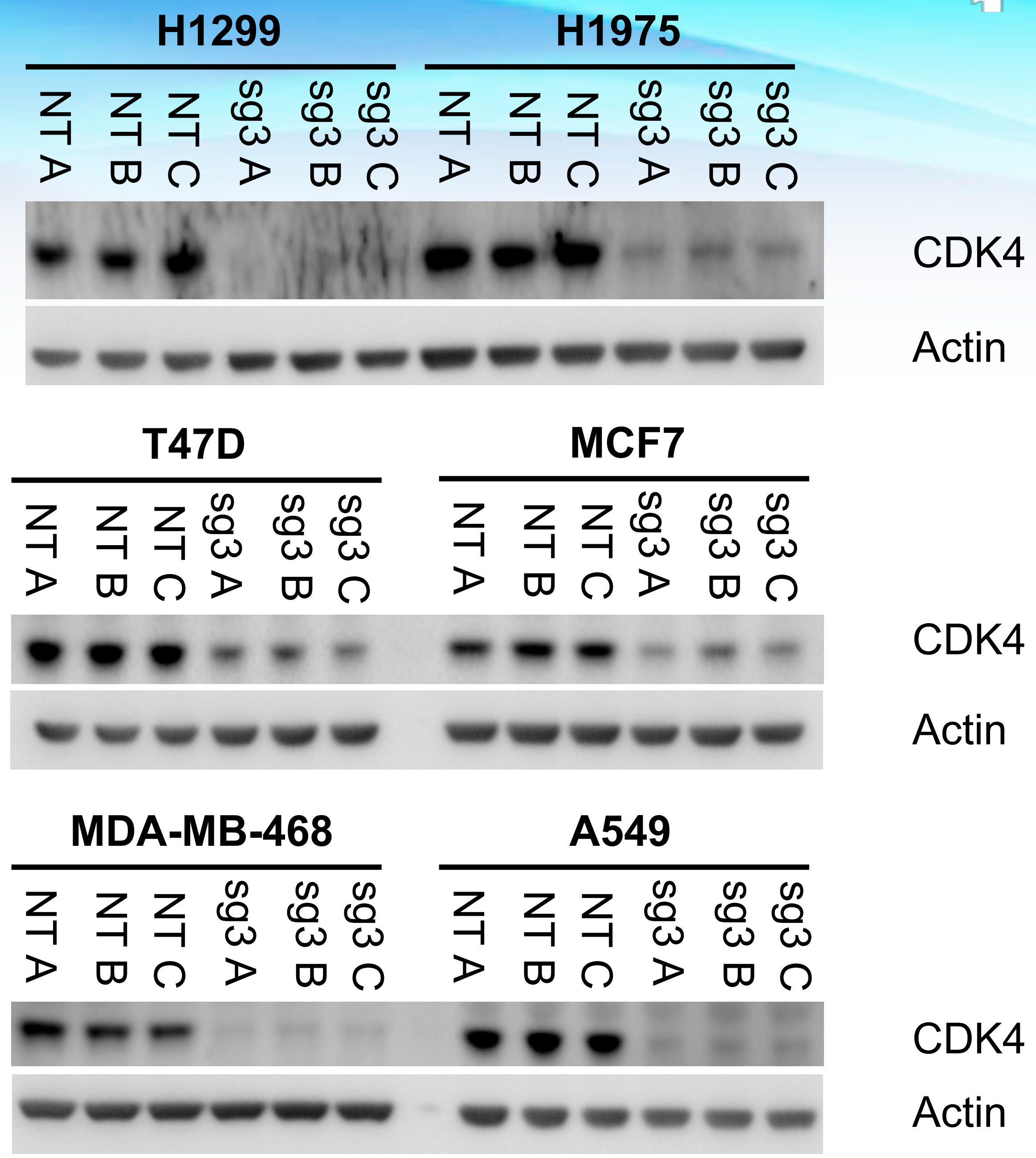

CDK4 KO vs NT Growth curves

WuXi AppTec

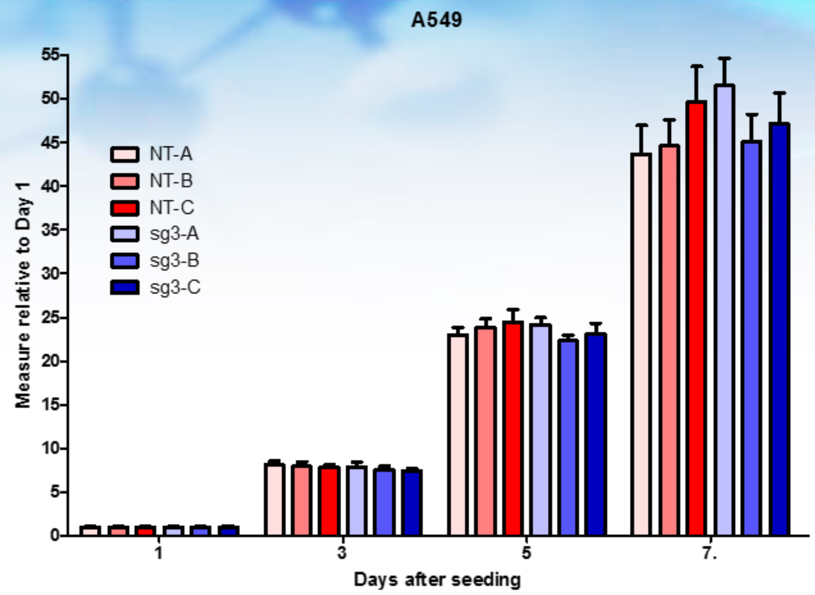
A549

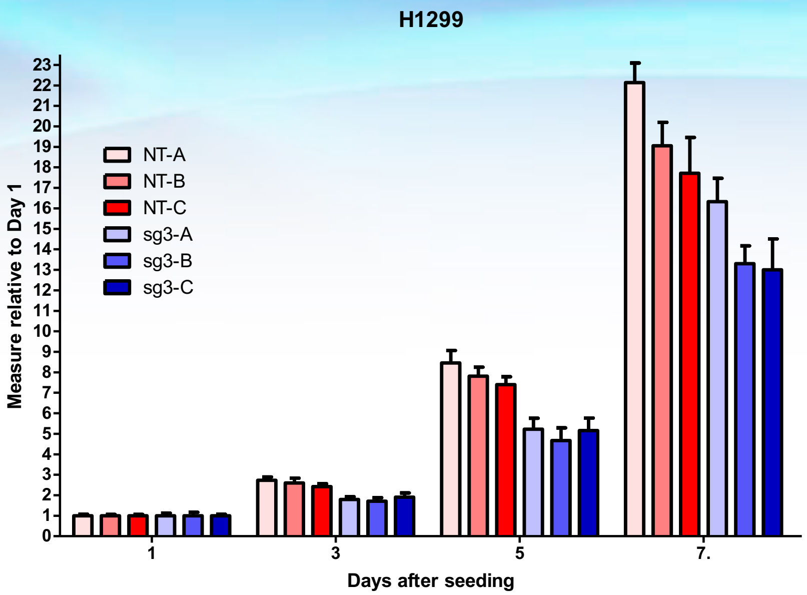
H1299

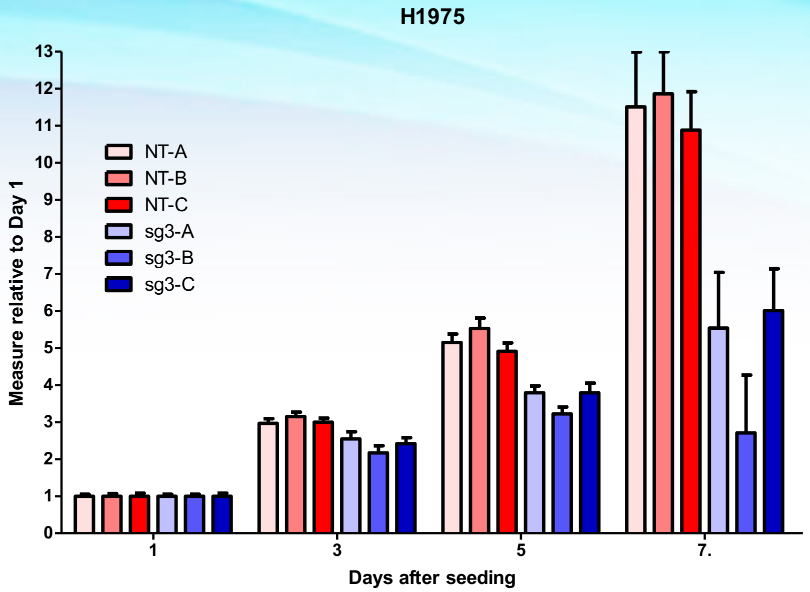
H1975

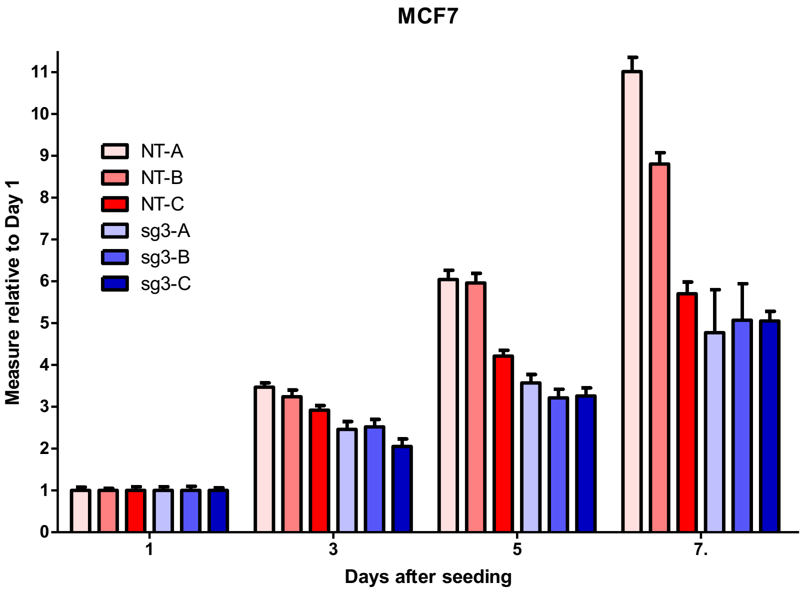
MCF7

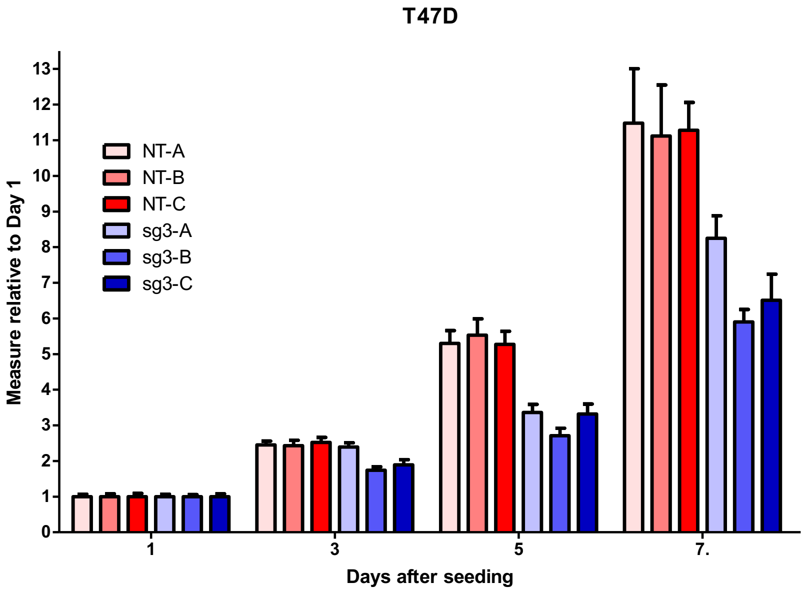
T47D

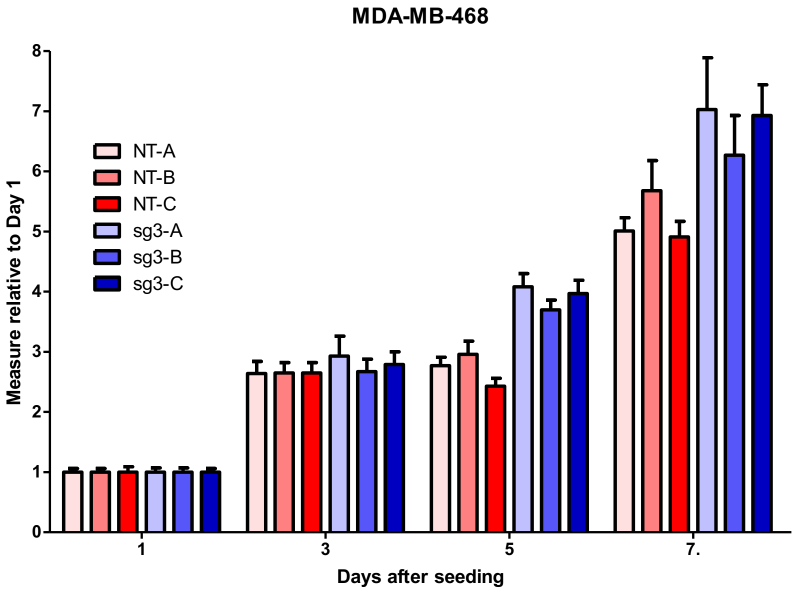
MDA-MB-468

Identifying Causal Drivers of Cardiovascular Disease: Hypertension, Vascular Hemorrhage, and Renal Failure

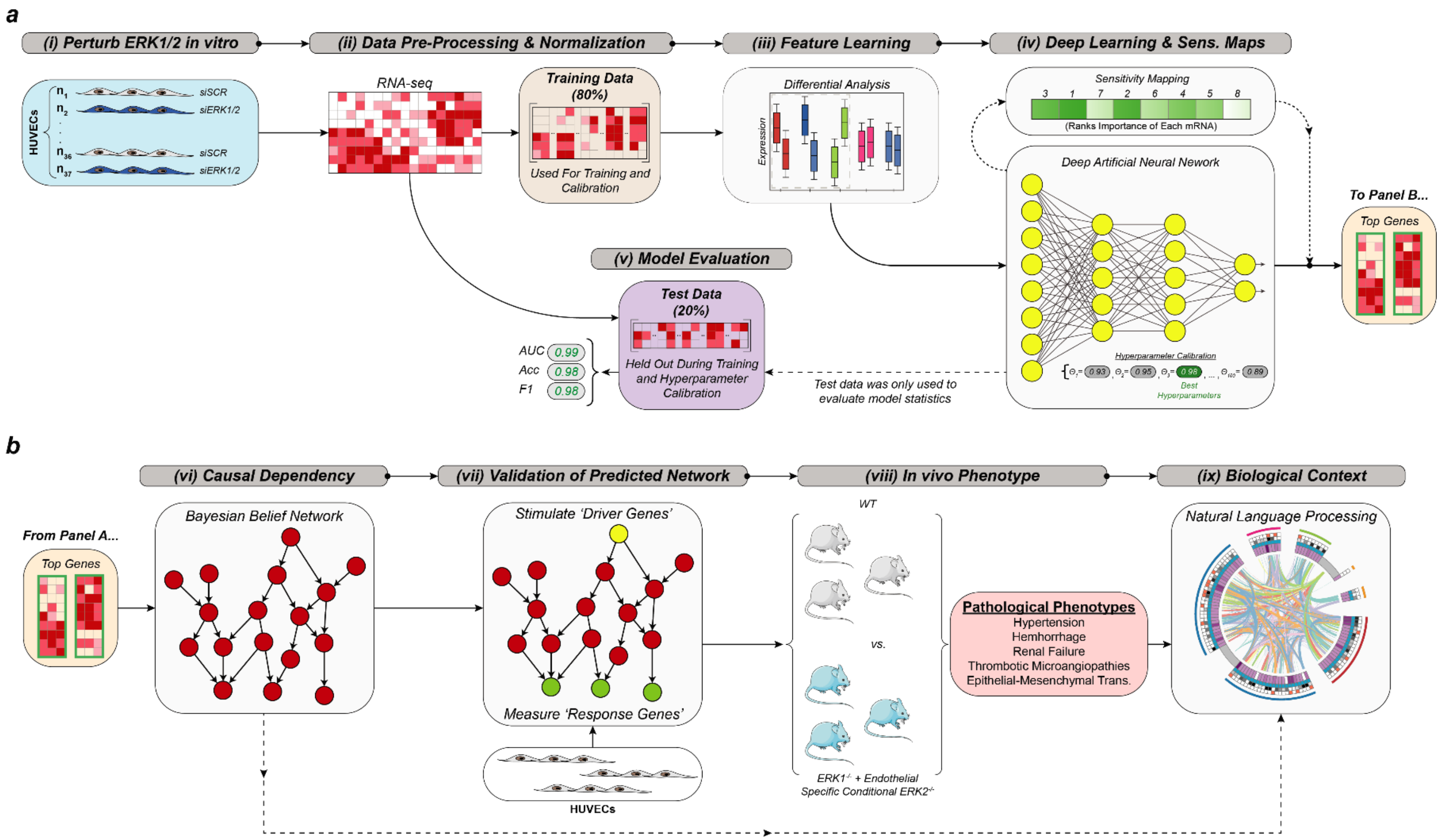

a
(i) Perturb ERK1/2 in vitro
HUVECs
n_1
siSCR
n_2
siERK1/2
n_{36}
siSCR
n_{37}
siERK1/2
(ii) Data Pre-Processing & Normalization
RNA-seq
Training Data (80%)
Used For Training and Calibration
(iii) Feature Learning
Differential Analysis
Expression
(iv) Deep Learning & Sens. Maps
Sensitivity Mapping
3 1 7 2 6 4 5 8
(Ranks Importance of Each mRNA)
Deep Artificial Neural Nework
Hyperparameter Calibration
{Θ_1= 0.93, Θ_2= 0.95, Θ_3= 0.98, ..., Θ_{100}= 0.89
Best Hyperparameters
To Panel B...
Top Genes
(v) Model Evaluation
Test Data (20%)
Held Out During Training and Hyperparameter Calibration
AUC 0.99
Acc 0.98
F1 0.98
Test data was only used to evaluate model statistics
b
From Panel A...
Top Genes
(vi) Causal Dependency
Bayesian Belief Network
(vii) Validation of Predicted Network
Stimulate 'Driver Genes'
Measure 'Response Genes'
HUVECs
(viii) In vivo Phenotype
WT
vs.
ERK1$^{-/-}$ + Endothelial Specific Conditional ERK2$^{-/-}$
Pathological Phenotypes
Hypertension
Hemhorrhage
Renal Failure
Thrombotic Microangiopathies
Epithelial-Mesenchymal Trans.
(ix) Biological Context
Natural Language Processing

Research Collaboration with Yale Cardiovascular Research Center
Deep Learning, BBN Analysis, and NLP of Single Cell RNA-seq Data

Identifying Causal Drivers of Cardiovascular Disease: Hypertension, Vascular Hemorrhage, and Renal Failure

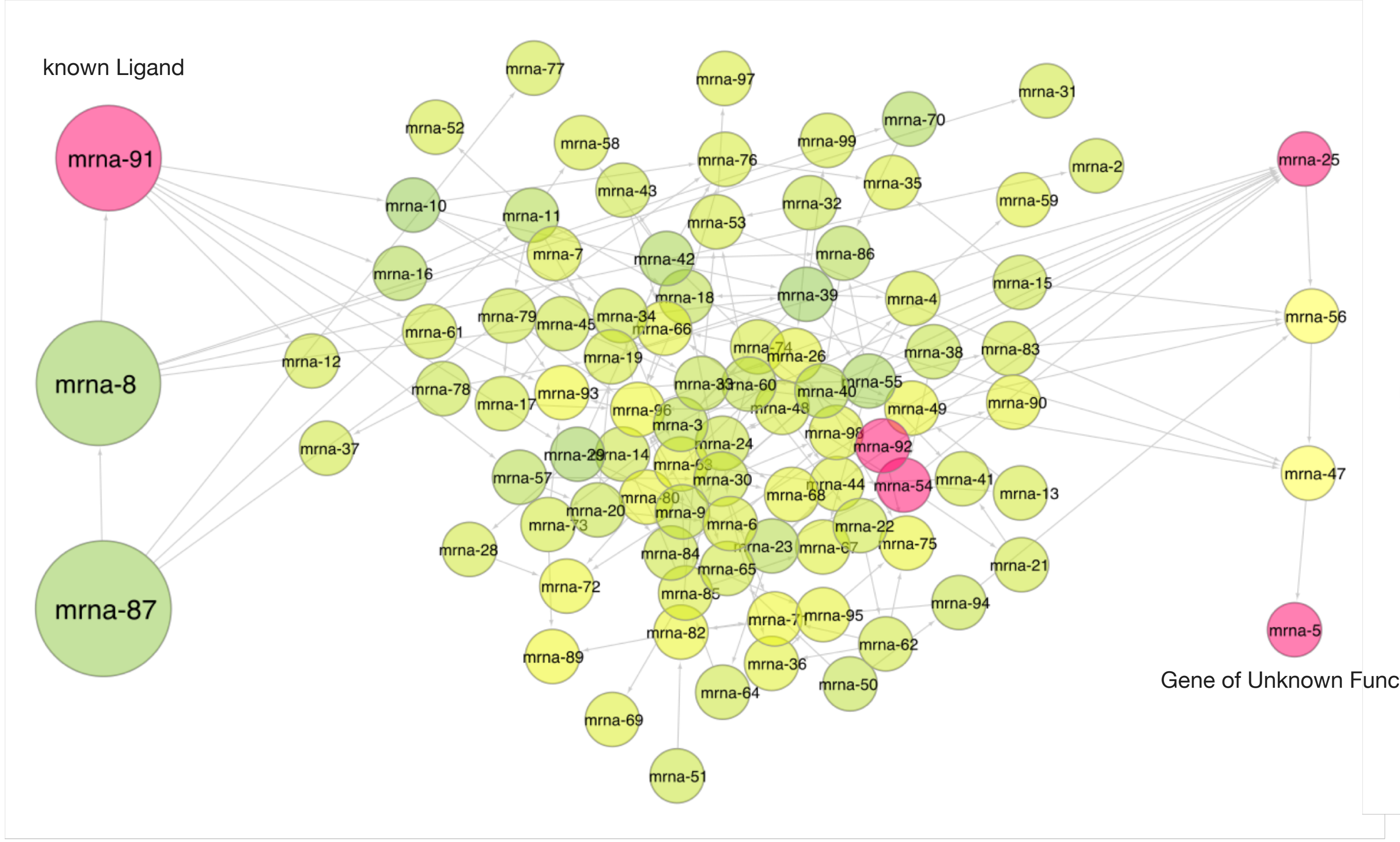

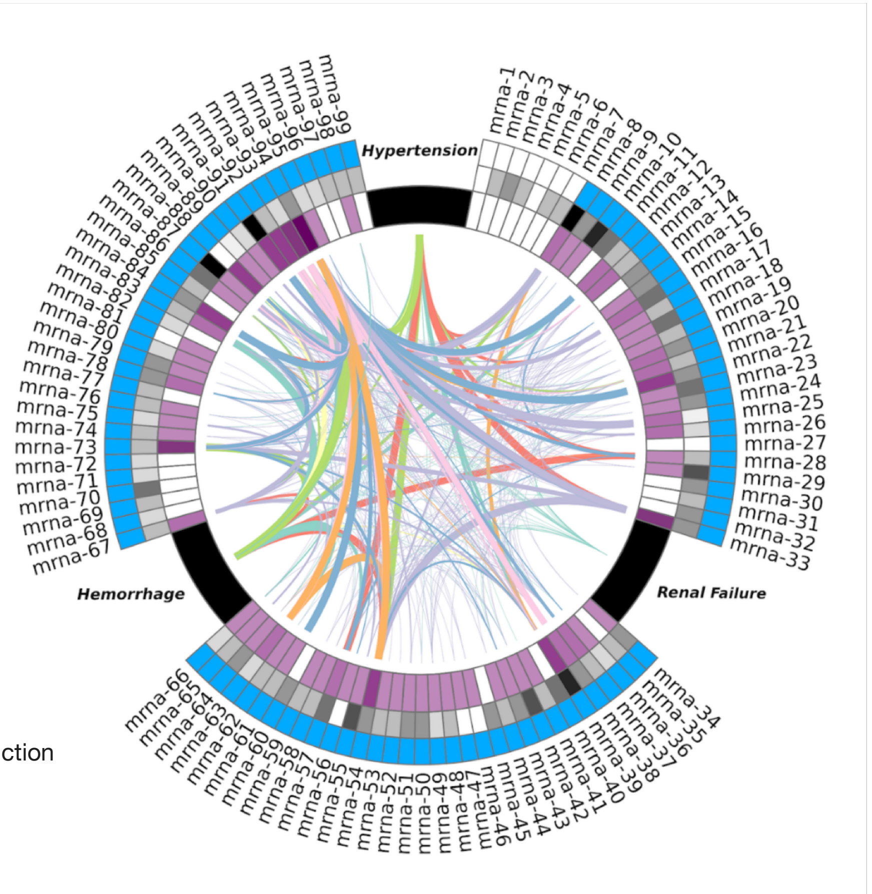

Research Collaboration with Yale Cardiovascular Research Center
Deep Learning, BBN Analysis, and NLP of Single Cell RNA-seq Data

Identifying Causal Drivers of Cardiovascular Disease: Aortic Aneurysm and Atherosclerosis

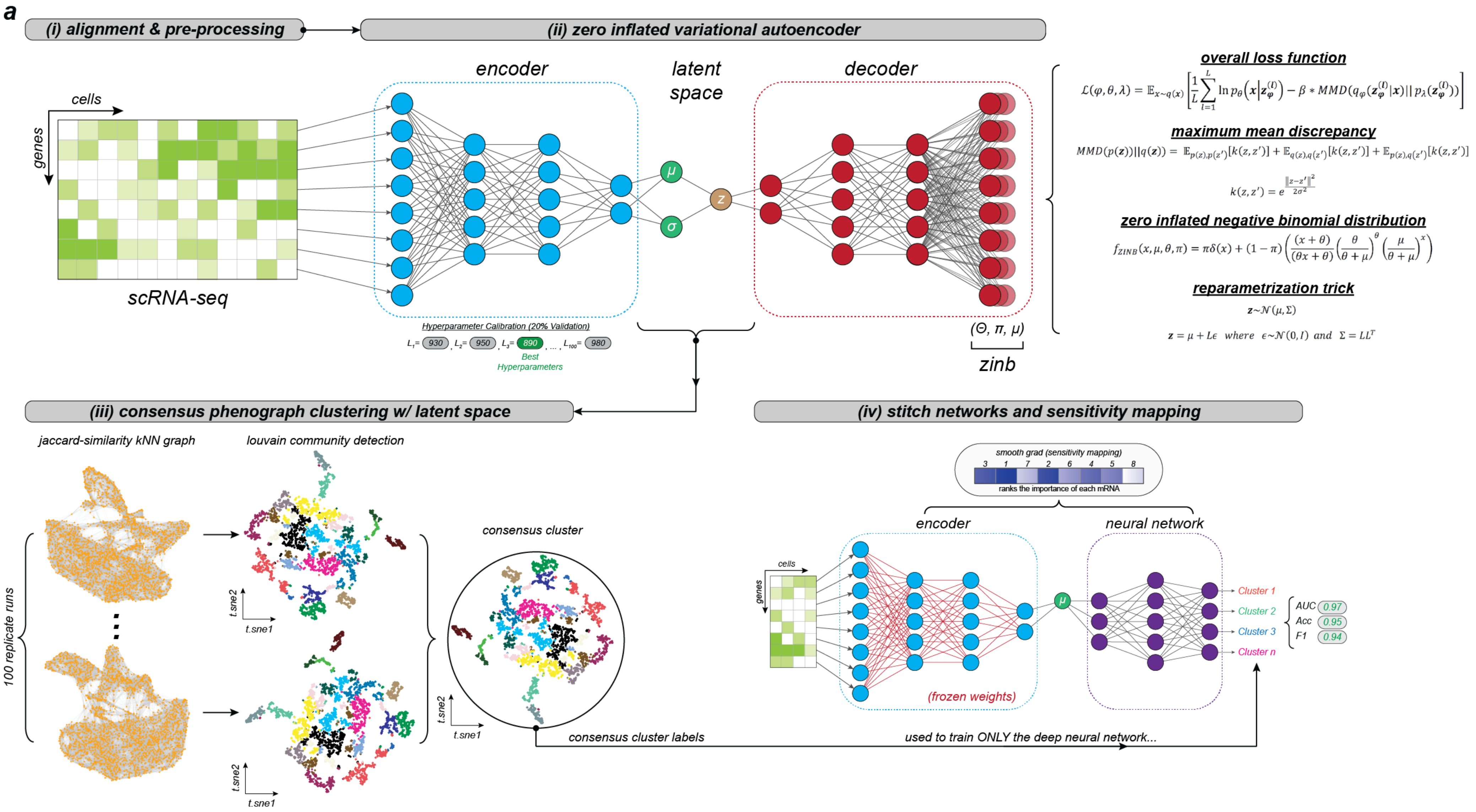

(i) alignment & pre-processing

(ii) zero inflated variational autoencoder

(iii) consensus phenograph clustering w/ latent space

(iv) stitch networks and sensitivity mapping

overall loss function

$$\mathcal{L}(\varphi,\theta,\lambda) = \mathbb{E}_{x\sim q(x)}\left[\frac{1}{L}\sum_{l=1}^{L} \ln p_\theta\left(\boldsymbol{x}\middle|\boldsymbol{z}_{\boldsymbol{\varphi}}^{(l)}\right) - \beta * MMD(q_\varphi(\boldsymbol{z}_{\boldsymbol{\varphi}}^{(l)}|\boldsymbol{x})\,||\,p_\lambda(\boldsymbol{z}_{\boldsymbol{\varphi}}^{(l)}))\right]$$

maximum mean discrepancy

$$MMD(p(\mathbf{z}))||q(\mathbf{z})) = \mathbb{E}_{p(z),p(z')}[k(z,z')] + \mathbb{E}_{q(z),q(z')}[k(z,z')] + \mathbb{E}_{p(z),q(z')}[k(z,z')]$$

$$k(z,z') = e^{\frac{\|z-z'\|^2}{2\sigma^2}}$$

zero inflated negative binomial distribution

$$f_{ZINB}(x,\mu,\theta,\pi) = \pi\delta(x) + (1-\pi)\left(\frac{(x+\theta)}{(\theta x+\theta)}\left(\frac{\theta}{\theta+\mu}\right)^{\theta}\left(\frac{\mu}{\theta+\mu}\right)^{x}\right)$$

reparametrization trick

$$\mathbf{z}\sim\mathcal{N}(\mu,\Sigma)$$

$$\mathbf{z} = \mu + L\epsilon \quad where \quad \epsilon\sim\mathcal{N}(0,I) \quad and \quad \Sigma = LL^T$$

Research Collaboration with Yale Cardiovascular Research Center
Deep Learning, BBN Analysis, and NLP of Single Cell RNA-seq Data

Identifying Causal Drivers of Cardiovascular Disease: Aortic Aneurysm

CyTOF (Cytometry by Time of Flight)

Vs.

Zero Inflated Variational Autoencoder (VAE) of Single Cell RNA-seq Data

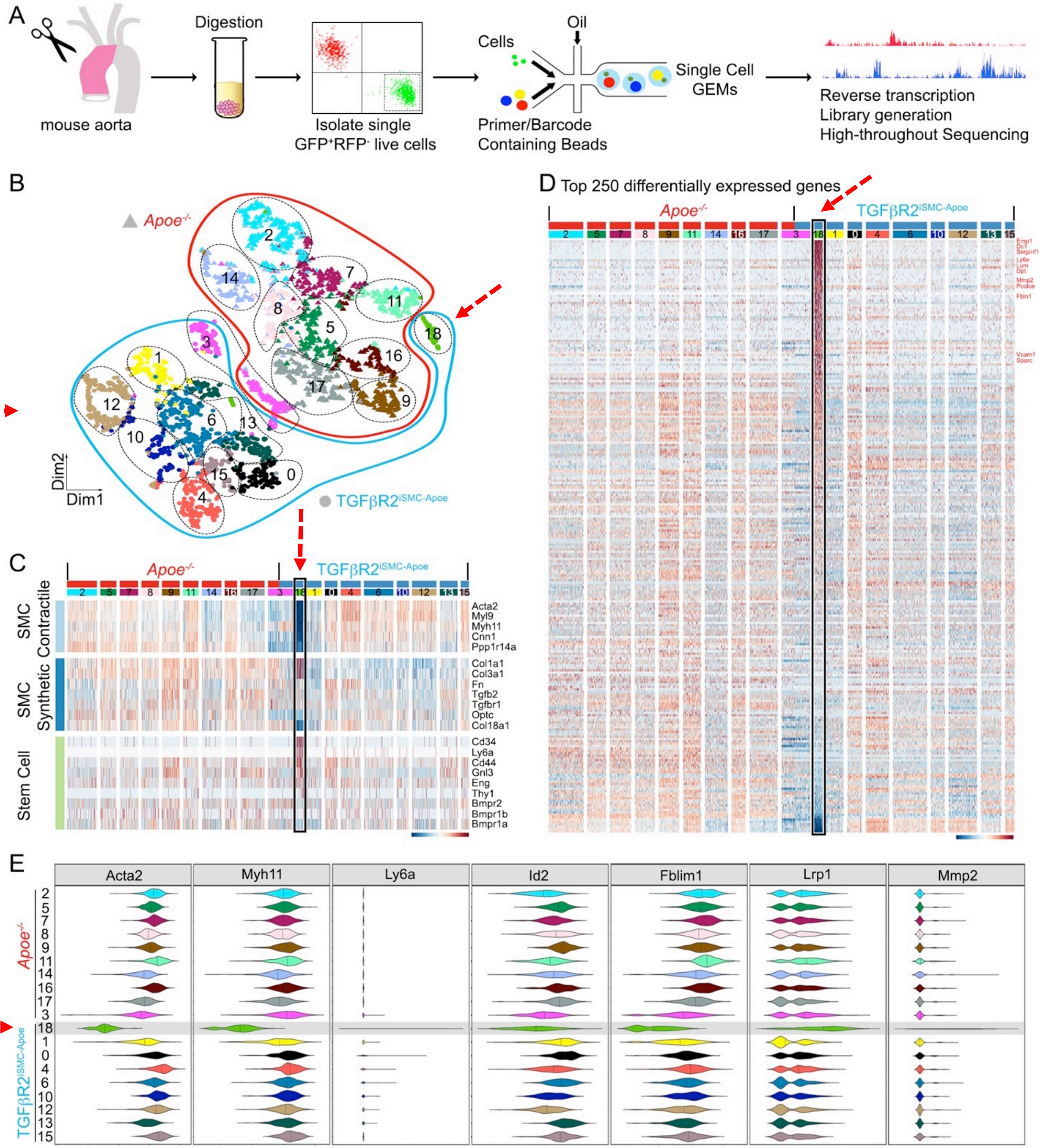

Cluster 18

Identifying Causal Drivers of Cardiovascular Disease:
Analysis of Cellular Differentiation in Aortic Aneurysm

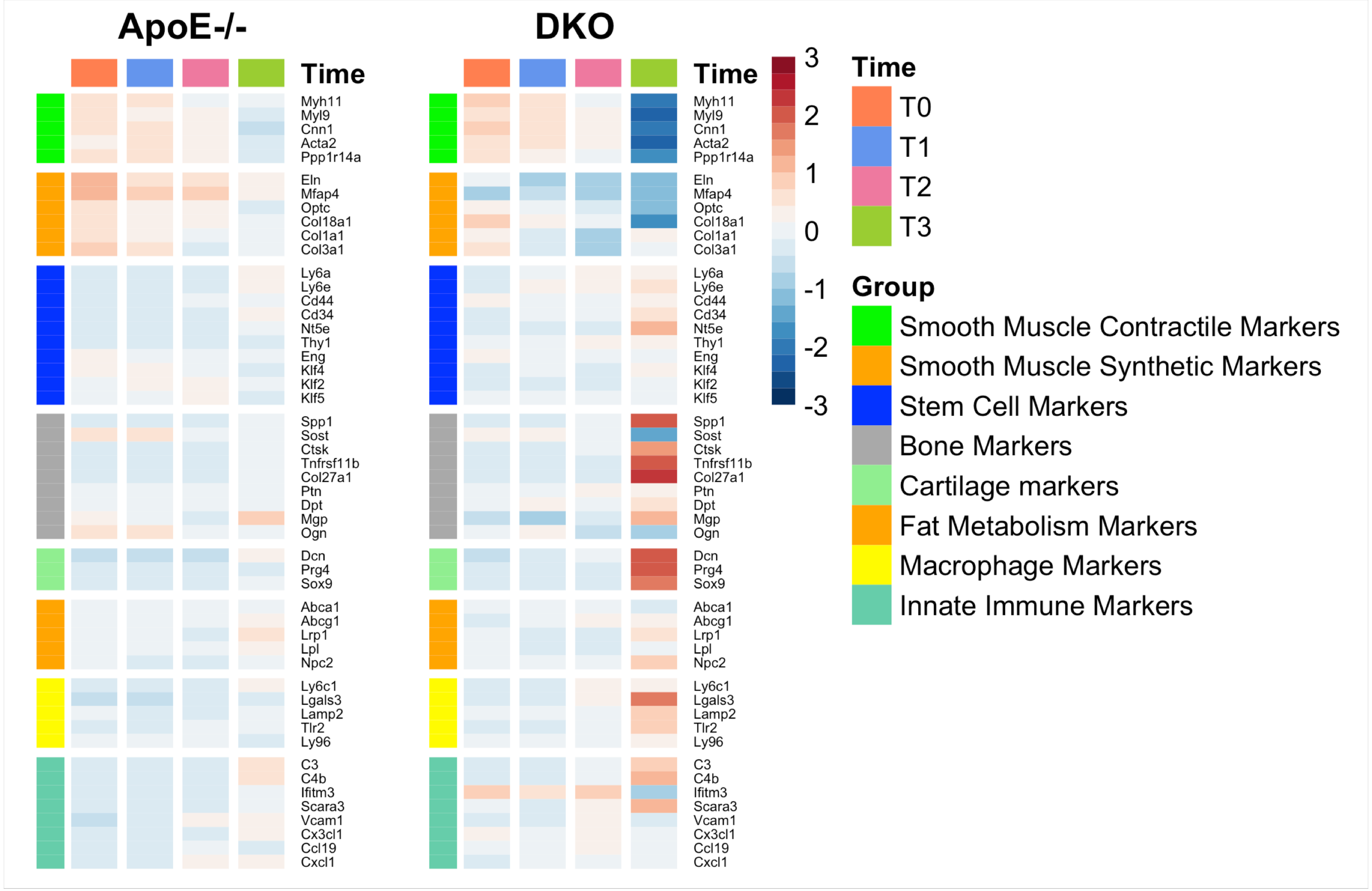

Identifying Causal Drivers of Cardiovascular Disease: Analysis of Cellular Differentiation in Aortic Aneurysm

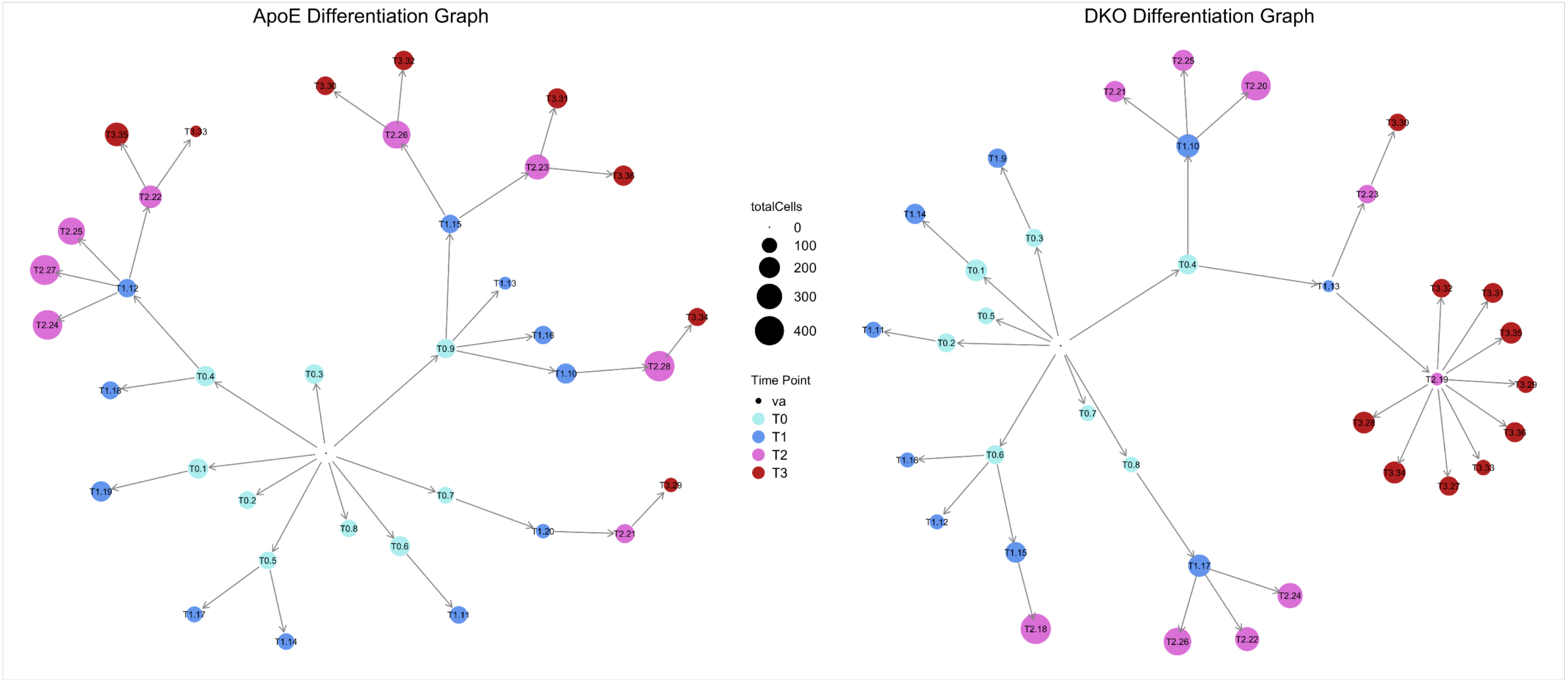

ApoE Differentiation Graph

DKO Differentiation Graph

Identifying Causal Drivers of Cardiovascular Disease: Analysis of Cellular Differentiation in Aortic Aneurysm

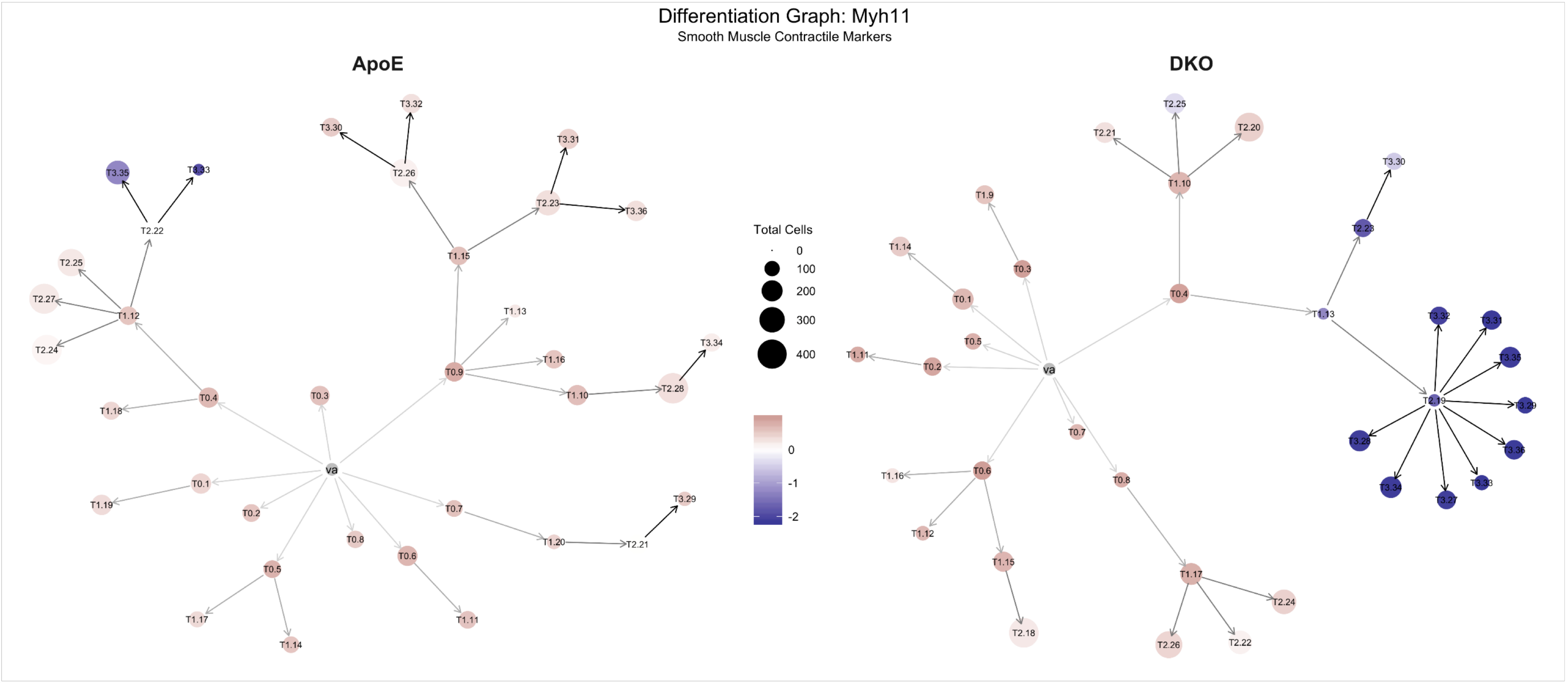

Identifying Causal Drivers of Cardiovascular Disease: Analysis of Cellular Differentiation in Aortic Aneurysm

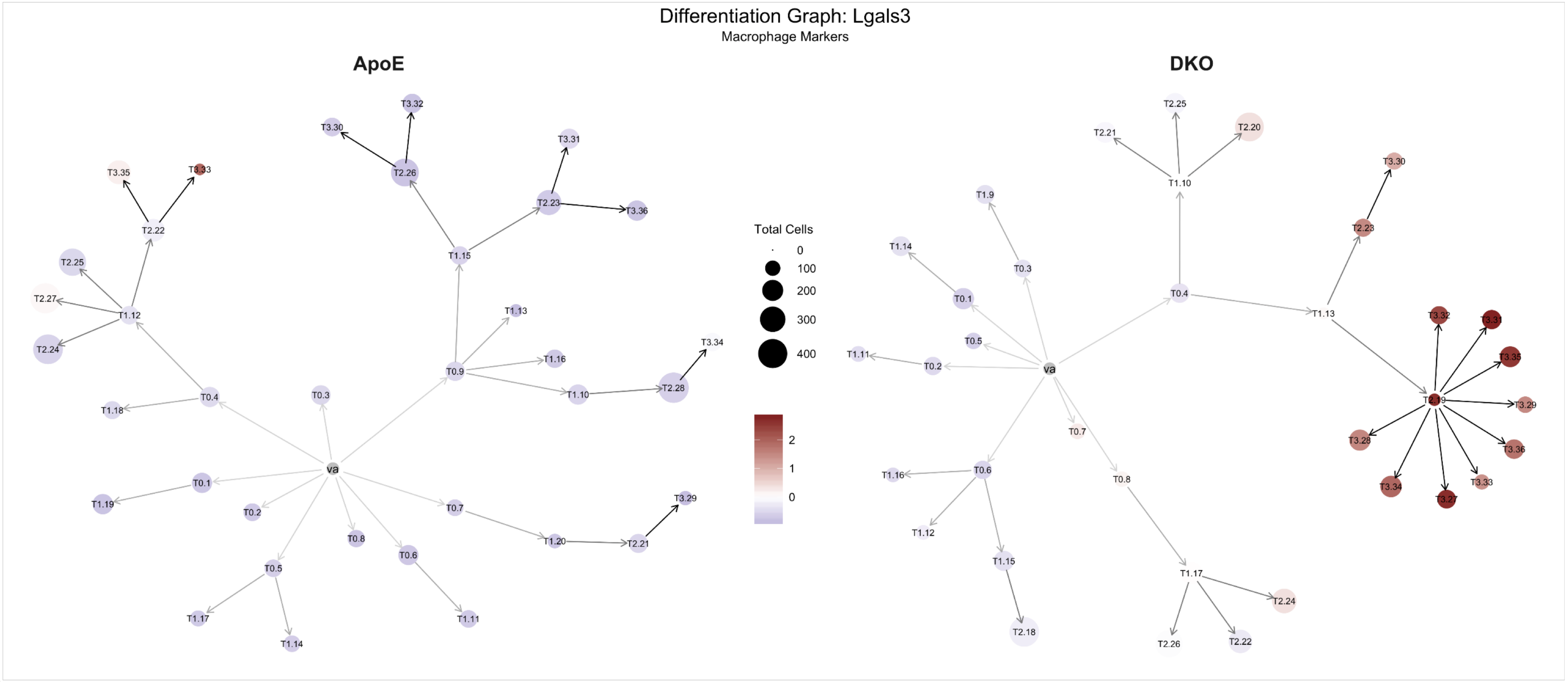

Quantum Machine Learning

- Quantum computing promises enhanced performance for many classes of problems associated with large datasets.

- We are in the process of replacing algorithmic components of our **Ensemble Computational Intelligence Strategy** with their respective quantum counterparts.

- Our first algorithm was a quantum hierarchical clustering (qHCl), based on a modified **Grover's algorithm**, a quantum **search algorithm** that runs quadratically faster than any equivalent classical algorithm.

- We have now built statistical quantum machine learning classifiers on both **IBM's universal quantum circuit architecture** and the **D-Wave Two X (DW2X) processor and DW2000Q Adiabatic quantum computer**. Our D-Wave qML algorithms achieve comparable, and in some cases slightly better, classification performance than their classical counterparts on **high-dimensional, multi-omic cancer data from the Cancer Genome Atlas (TCGA)**.

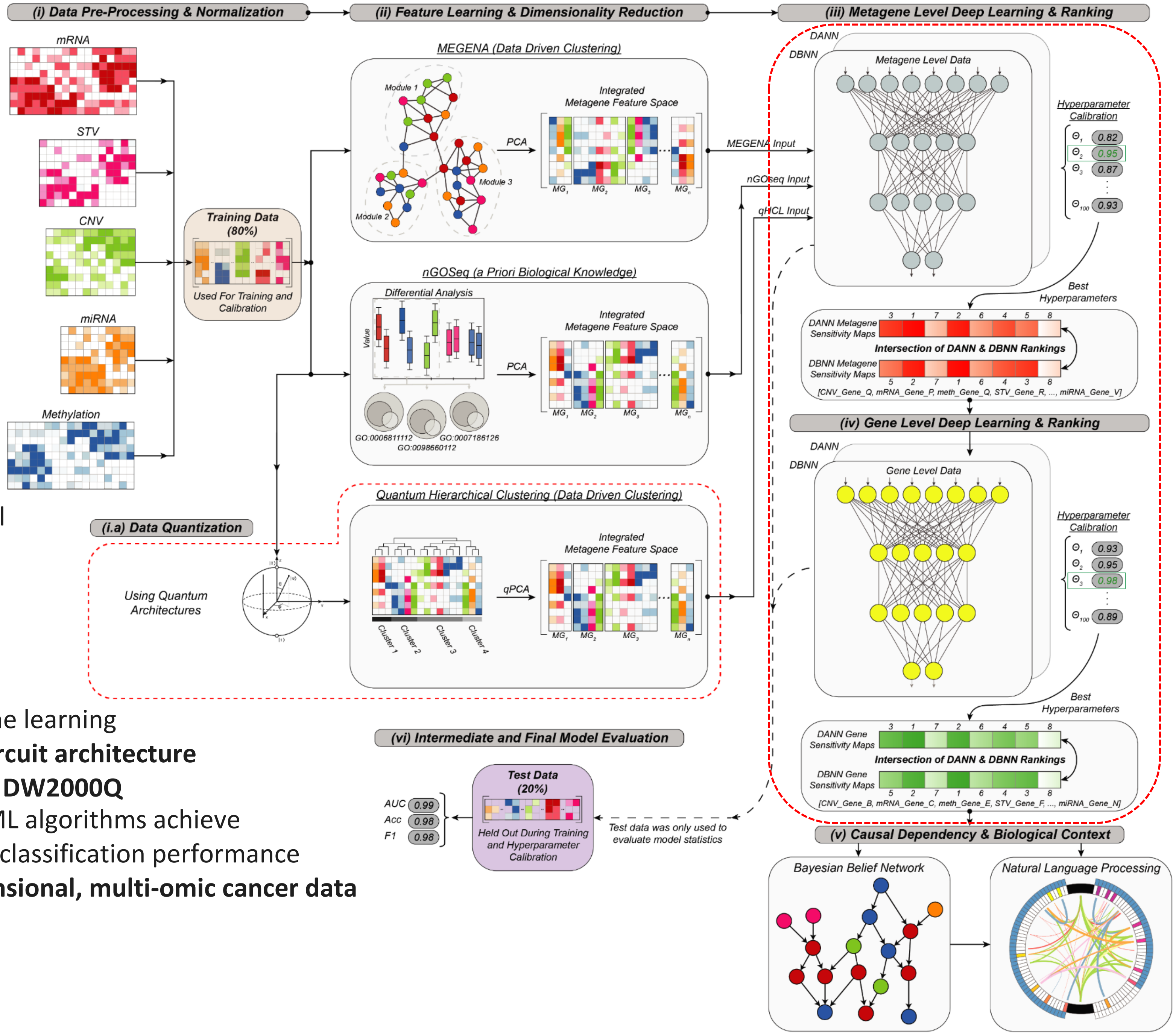

(i) Data Pre-Processing & Normalization
mRNA
STV
CNV
miRNA
Methylation
Training Data (80%)
Used For Training and Calibration
(i.a) Data Quantization
Using Quantum Architectures
(ii) Feature Learning & Dimensionality Reduction
MEGENA (Data Driven Clustering)
Module 1
Module 2
Module 3
PCA
Integrated Metagene Feature Space
MG_1
MG_2
MG_3
MG_n
nGOSeq (a Priori Biological Knowledge)
Differential Analysis
Value
GO:0006811112
GO:0007186126
GO:0098660112
PCA
Integrated Metagene Feature Space
MG_1
MG_2
MG_3
MG_n
Quantum Hierarchical Clustering (Data Driven Clustering)
Cluster 1
Cluster 2
Cluster 3
Cluster 4
qPCA
Integrated Metagene Feature Space
MG_1
MG_2
MG_3
MG_n
MEGENA Input
nGOseq Input
qHCL Input
(iii) Metagene Level Deep Learning & Ranking
DANN
DBNN
Metagene Level Data
Hyperparameter Calibration
Θ_1 0.82
Θ_2 0.95
Θ_3 0.87
Θ_{100} 0.93
Best Hyperparameters
DANN Metagene Sensitivity Maps
3 1 7 2 6 4 5 8
Intersection of DANN & DBNN Rankings
DBNN Metagene Sensitivity Maps
5 2 7 1 6 4 3 8
[CNV_Gene_Q, mRNA_Gene_P, meth_Gene_Q, STV_Gene_R, ..., miRNA_Gene_V]
(iv) Gene Level Deep Learning & Ranking
DANN
DBNN
Gene Level Data
Hyperparameter Calibration
Θ_1 0.93
Θ_2 0.95
Θ_3 0.98
Θ_{100} 0.89
Best Hyperparameters
DANN Gene Sensitivity Maps
3 1 7 2 6 4 5 8
Intersection of DANN & DBNN Rankings
DBNN Gene Sensitivity Maps
5 2 7 1 6 4 3 8
[CNV_Gene_B, mRNA_Gene_C, meth_Gene_E, STV_Gene_F, ..., miRNA_Gene_N]
(v) Causal Dependency & Biological Context
Bayesian Belief Network
Natural Language Processing
(vi) Intermediate and Final Model Evaluation
AUC 0.99
Acc 0.98
F1 0.98
Test Data (20%)
Held Out During Training and Hyperparameter Calibration
Test data was only used to evaluate model statistics

Binomial Classification of Tumor Molecular Subtypes
Quantum Machine Learning

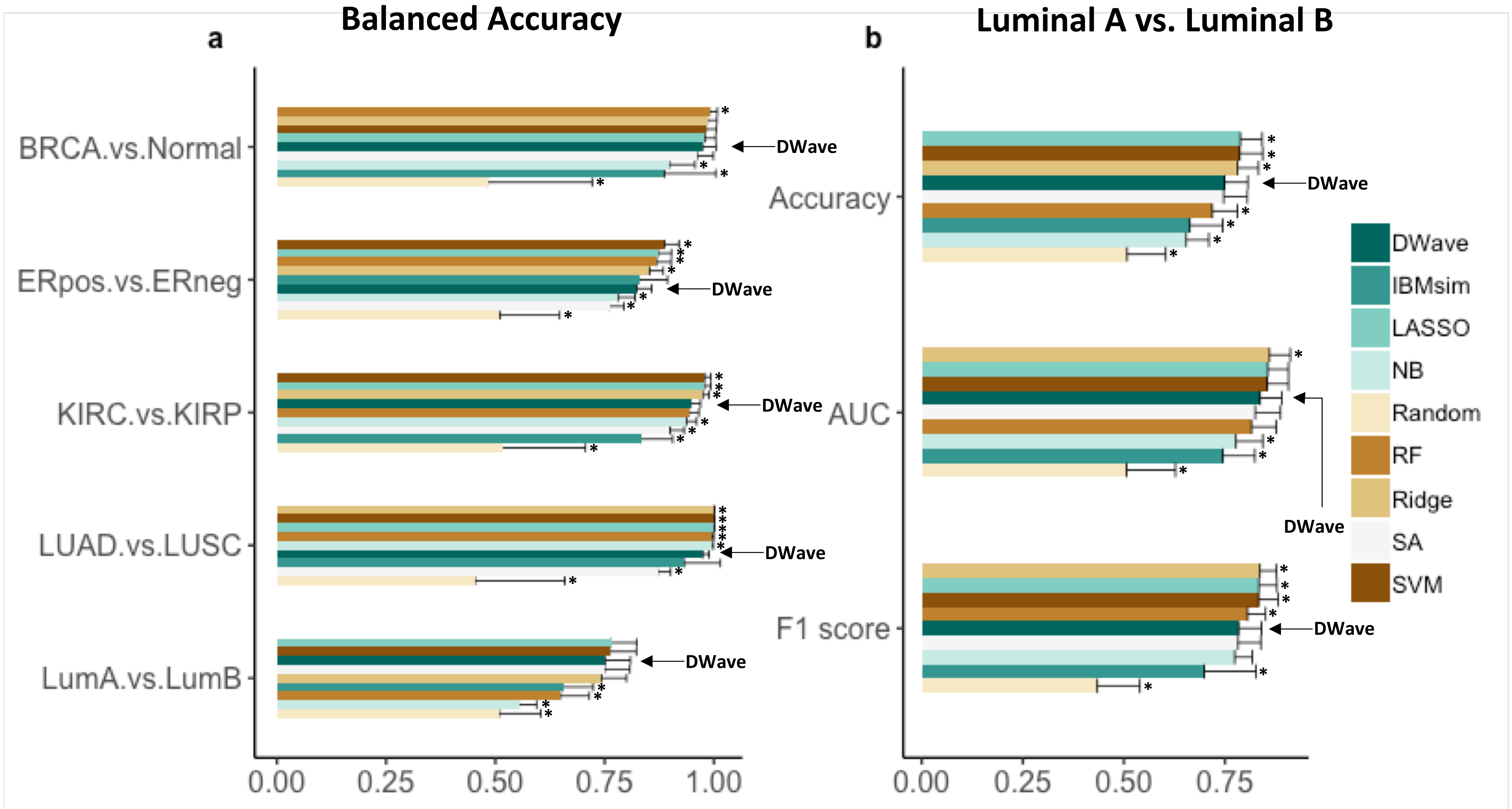

Binomial Classification of Tumor Molecular Subtypes
Luminal A vs. Luminal B Human Breast Cancers

DWave

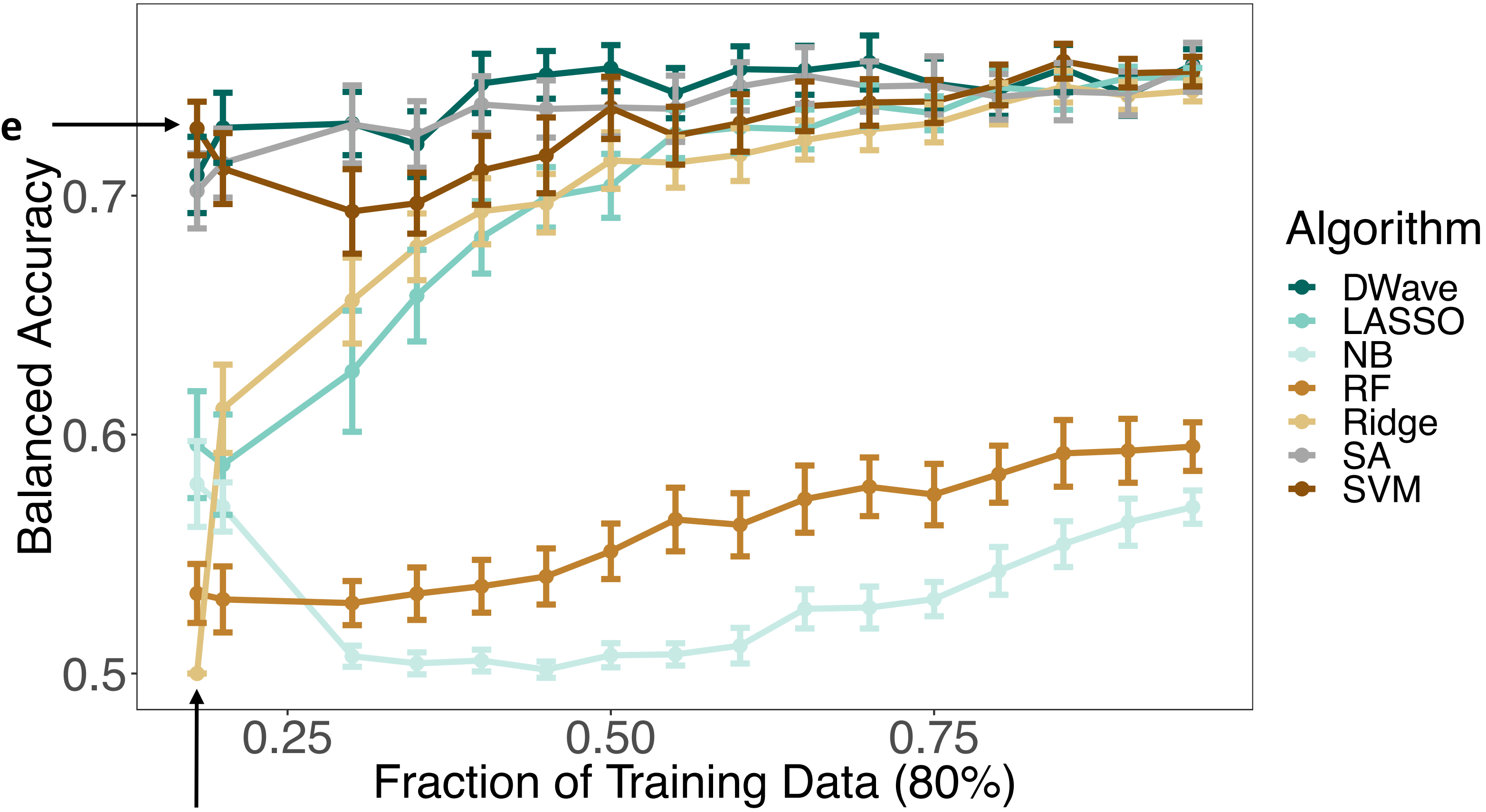

34 Patient Samples

LumA vs. LumB Status	
Tumor Samples	231
Luminal A	119
Luminal B	112
Train	185
Test	46

Binomial Classification of Tumor Molecular Subtypes: Luminal A vs. Luminal B Human Breast Cancers

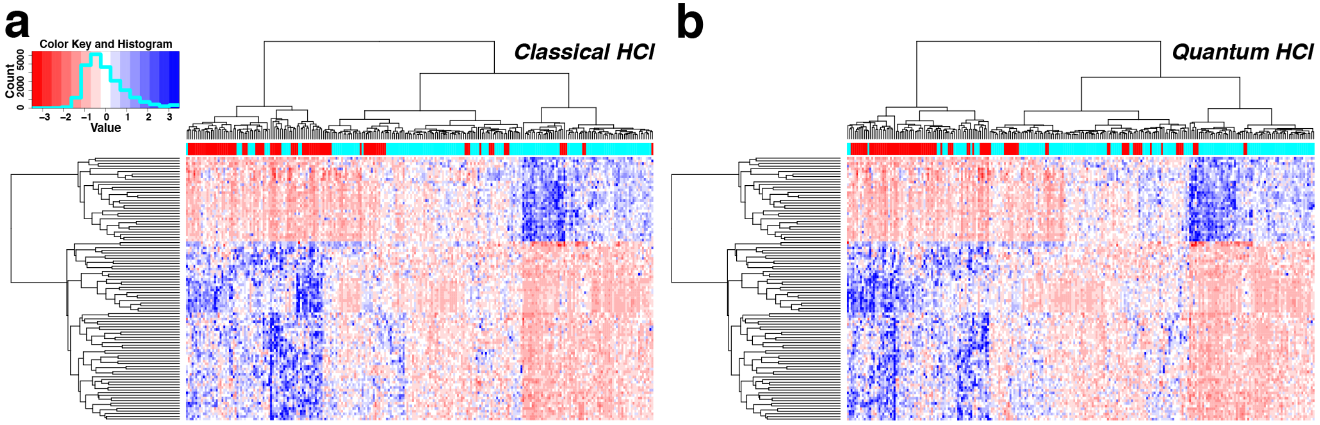

LumA vs. LumB Status	
Tumor Samples	231
Luminal A	119
Luminal B	112
Train	185
Test	46

*Quantum and classical trees are 88% concordant based on the standard Robinson–Foulds metric

*qHCL - Durr-Hoyer method based on a modified Grover's search algorithm with Euclidean distance and Ward linkage

*qHCL ran on a IBM quantum simulator using 19 qubits

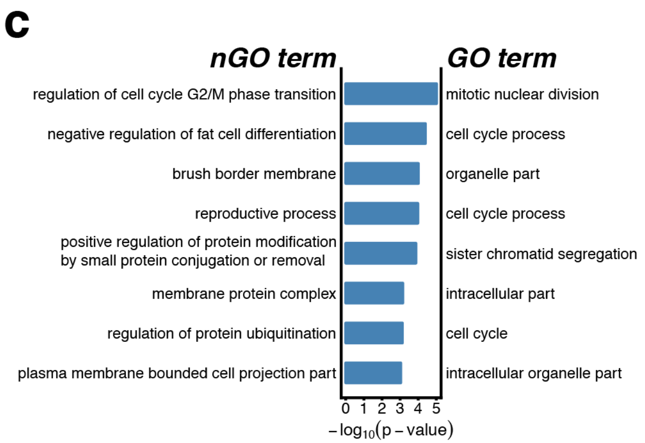

Functional Enrichment

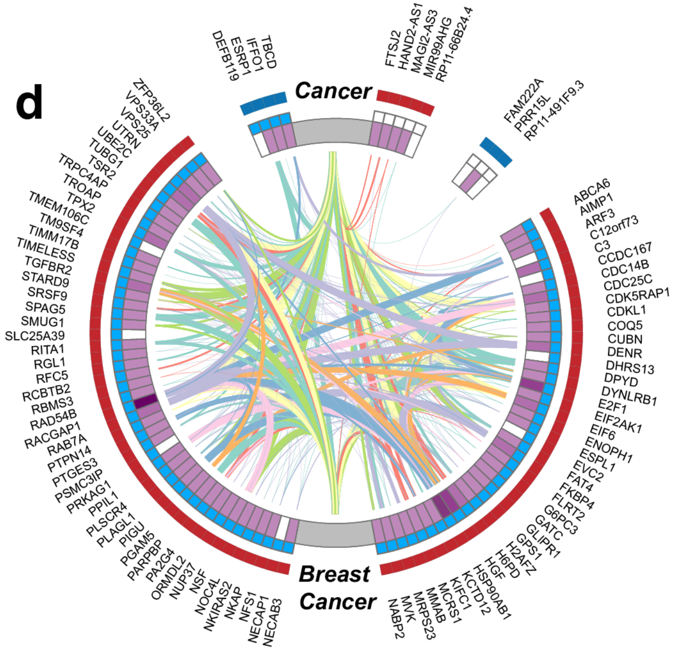

Natural Language Processing

*Outer red band: mrna data
*Outer blue band: methylation data
*Inner blue band: genes of known function

Multinomial Classification of Human Cancer Types
Quantum Machine Learning

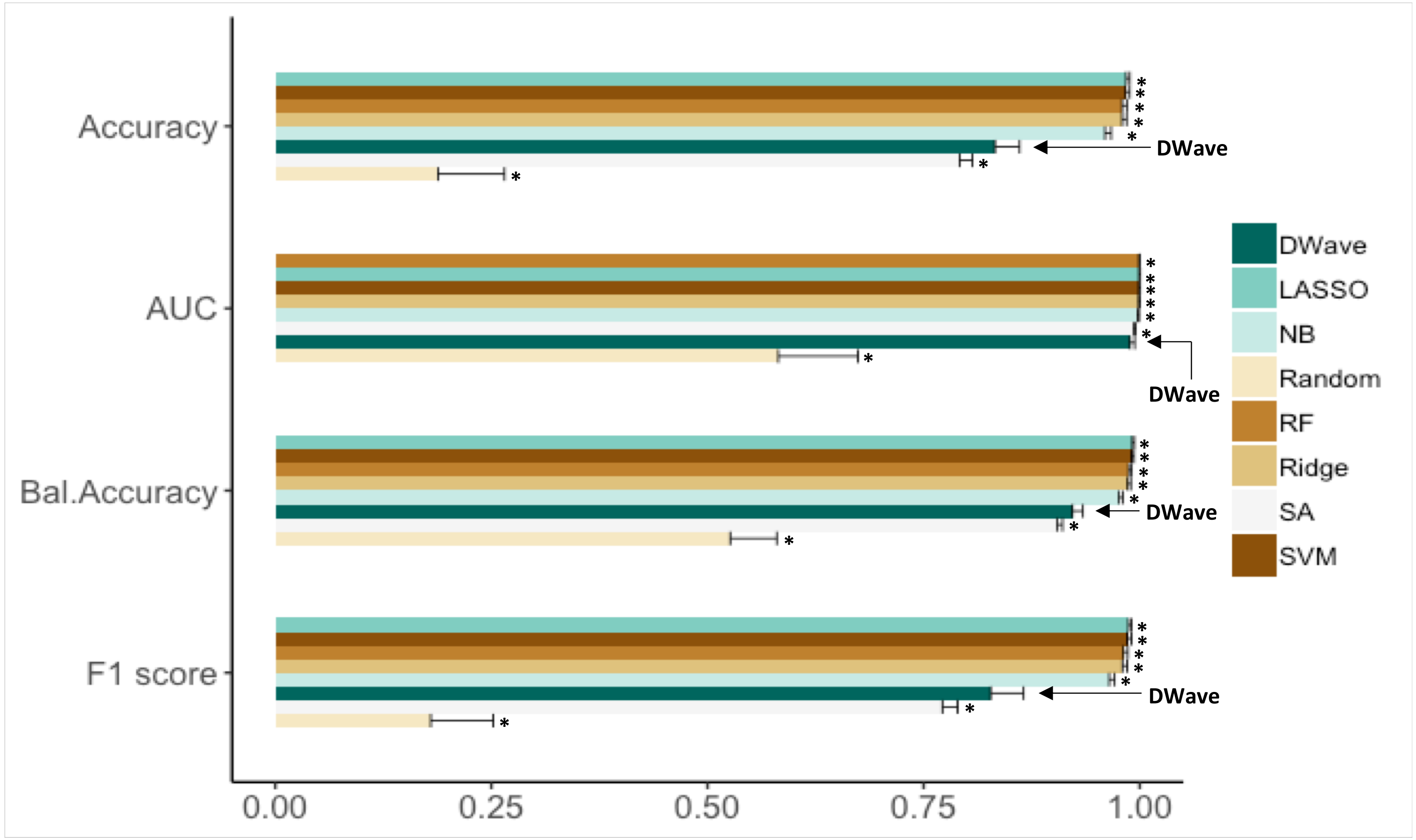

Human Cancer Types	Sample Number
Liver Hepatocellular Carcinoma	**358**
Breast cancer	**1006**
Brain Lower Grade Glioma	**499**
Colon Adenocarcinoma/Rectum Adenocarcinoma	**551**
Kidney Cancer	**611**
Lung Cancer	**962**
Total	**3987**
Train	**3190**
Test	**797**

Advanced Artificial Intelligence Research Laboratory

Academic and Industry Research Collaborations

Harvard Medical School

Professor Chris Walsh
Chief of Genetics and Genomics

University of Oxford

Professor Chris Holmes
Computational Statistics and Machine Learning

University of Southern California

Professor Daniel Lidar
Quantum Computing and Quantum Machine Learning

University of Toronto

Professor Alán Aspuru-Guzik
Quantum Chemistry and Chemical Biology

WuXi AppTec Oncology

Fabrice Alphonse

Yale University School of Medicine

Professor Michael Simons
Director of Yale Cardiovascular Research Center

Professor Karen Hirschi
Yale Cardiovascular Research Center

Acknowledgements

WuXi NextCODE

- Jeff Gulcher
- Richard Williams
- Rob Brainin
- Hákon Guðbjartsson
- Hongye Sun
- Jim Lund
- Shannon Bailey
- Simonne Longerich

WuXi NextCODE Advanced A.I. Research Laboratory

- Chandri Yandava
- Sharvari Gujja
- Joe White
- Sweta Bajaj
- Javier Baylon
- Omar Gamel
- Prasad Reddy
- Jose Malagon Lopez

Boston Children's Hospital Harvard Medical School

- Chris Walsh
- Mike Lodato

Cardiovascular Research Center Yale University Medical School

- Mike Simons
- Pengchun Yu

University of Oxford

- Chris Holmes

University of Tennessee

- Hao Chen

APPENDIX

14 DECEMBER | TWO THOUSAND EIGHTEEN

Modeling Human Breast Cancer – High Generalizability

Molecular Subtypes using Somatic Tumor Variants (STVs) and mRNA

Novel deepCODE pathway-based integration approach classifies tumor subtypes and tumor vs. normal at high accuracy
This classification reveals key mutated and expressed genes/pathways.

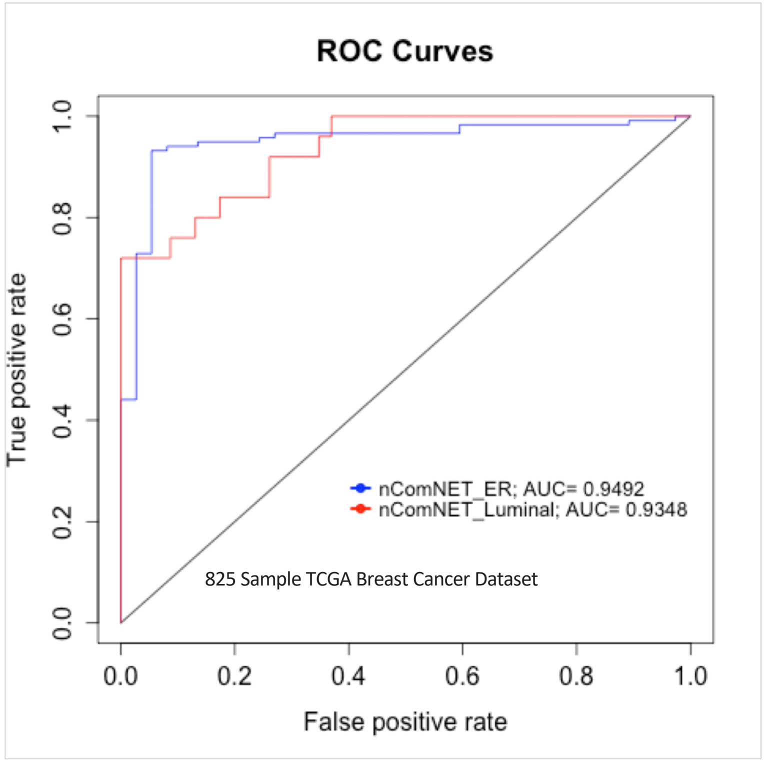

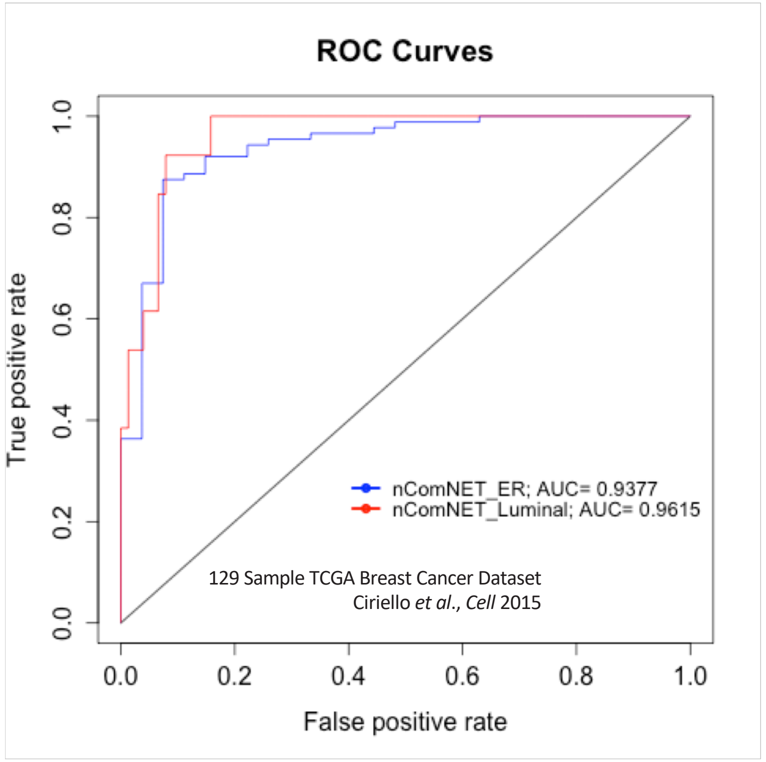

ER- vs. ER+ Breast Tumor Classification with 0.95 accuracy
2 Mutated Pathways (10 genes); 5 Aberrant Expression Pathways (146 genes)

Luminal A vs. B Breast Tumor Classification with 0.94 accuracy
4 Mutated Pathways (172 genes); 8 Aberrant Expression Pathways (72 genes)

Cross-Platform Analysis: RNA-seq to DNA Microarray – High Generalizability

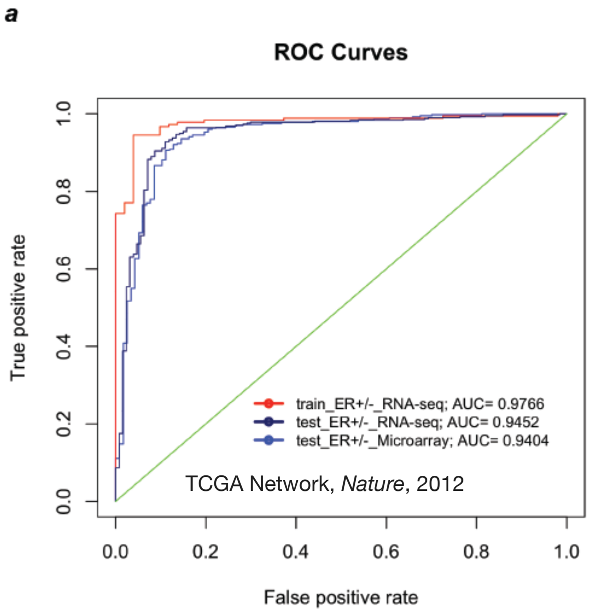

TCGA Network, *Nature*, 2012

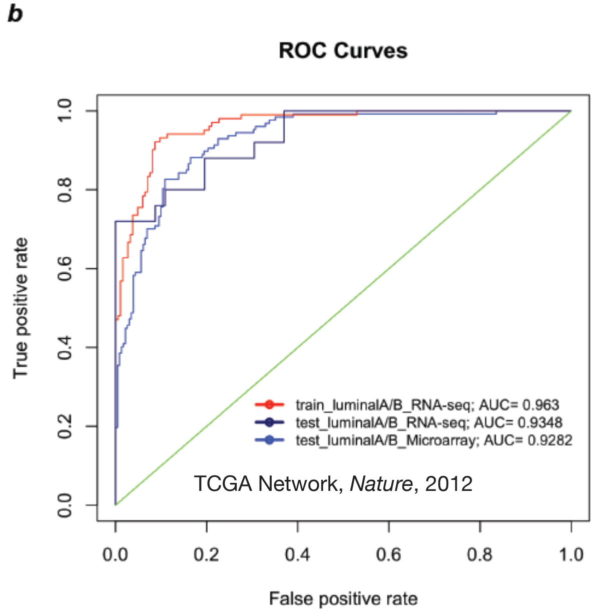

TCGA Network, *Nature*, 2012

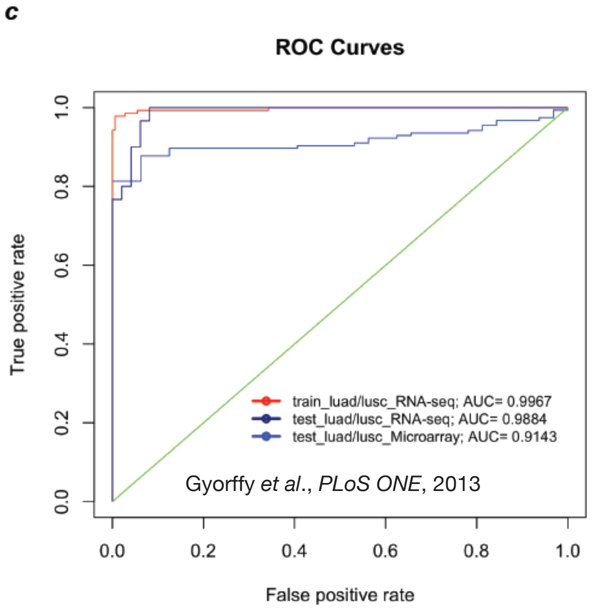

Gyorffy *et al*., *PLoS ONE*, 2013

a. ER- vs. ER+ Classification with AUC = 0.95

5 Aberrant Expression Pathways (146 genes)

b. Luminal A vs. B Classification with AUC = 0.94

8 Aberrant Expression Pathways (72 genes)

c. LUAD vs. LUSC Classification with AUC = 0.98

9 Aberrant Expression Pathways (60 genes)

Our deep learning approach to classification of TCGA tumor Types is far superior to traditional machine learning methods (LASSO)

DeepCODE Deep Learning vs. LASSO Machine Learning Multinomial Regression Models on 28 TCGA cancer types

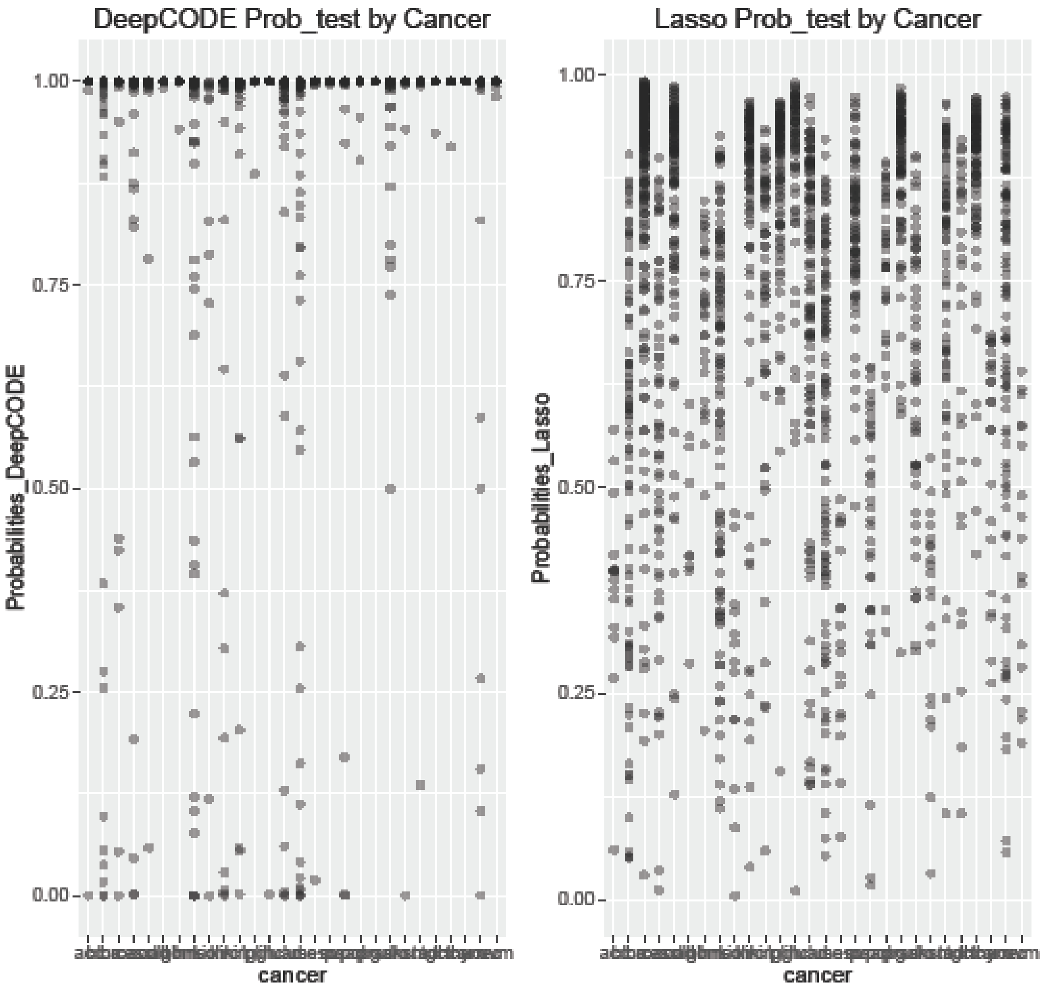

Multinomial Human Cancer Classification:

Trained: 7,618 RNA-seq samples; Tested:1,889 RNA-seq samples

True Positive Probability Distributions per Cancer type

Note: deepCODE Model Calls True Positives with far greater confidence

Brain projects come together pp. 11 & 42
The hidden force behind this year's El Niño p. 22
Reducing fuel fire hazards pp. 32 & 72
Science
$10
2 OCTOBER 2015
sciencemag.org
AAAS
Brain neurons diverge
Mutations reveal developmental pathways pp. 37 & 94

Lodato *et al.*, *Science* 2015
Lodato *et al.*, *Science* 2017

NEURODEVELOPMENT

Somatic mutation in single human neurons tracks developmental and transcriptional history

Michael A. Lodato,[1]* Mollie B. Woodworth,[1]* Semin Lee,[2]* Gilad D. Evrony,[1] Bhaven K. Mehta,[1] Amir Karger,[3] Soohyun Lee,[2] Thomas W. Chittenden,[3,4]† Alissa M. D'Gama,[1] Xuyu Cai,[1]‡ Lovelace J. Luquette,[2] Eunjung Lee,[2,5] Peter J. Park,[2,5]§ Christopher A. Walsh[1]§

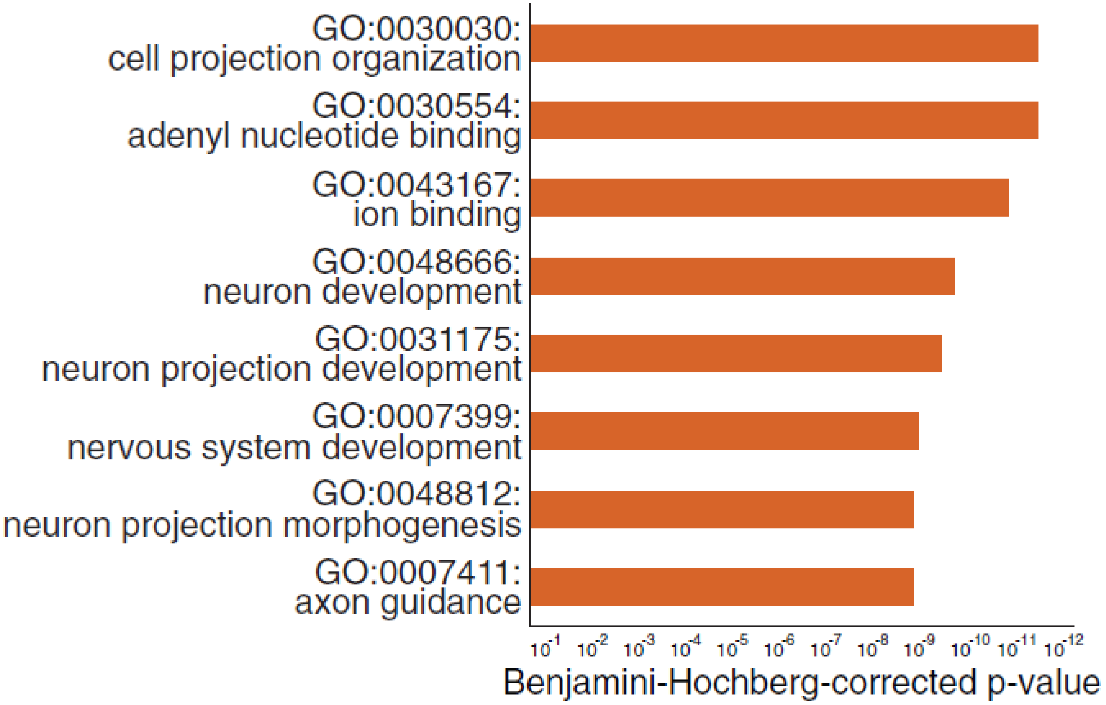

WuXiNextCODE

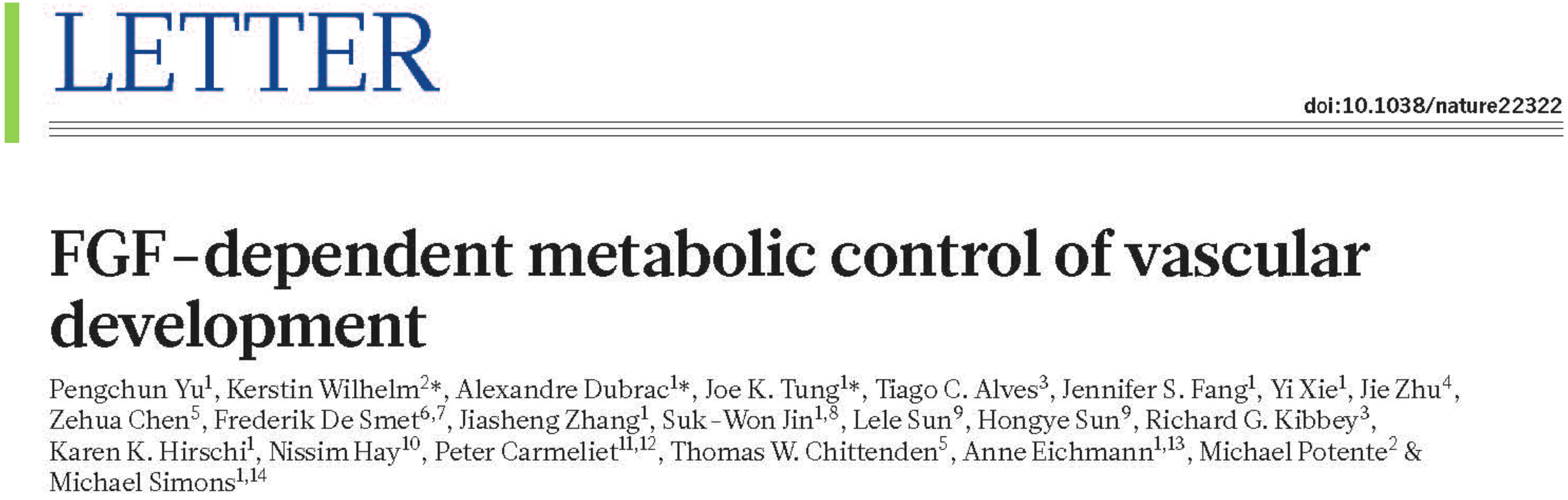

LETTER

doi:10.1038/nature22322

FGF-dependent metabolic control of vascular development

Pengchun Yu[1], Kerstin Wilhelm[2]*, Alexandre Dubrac[1]*, Joe K. Tung[1]*, Tiago C. Alves[3], Jennifer S. Fang[1], Yi Xie[1], Jie Zhu[4], Zehua Chen[5], Frederik De Smet[6,7], Jiasheng Zhang[1], Suk-Won Jin[1,8], Lele Sun[9], Hongye Sun[9], Richard G. Kibbey[3], Karen K. Hirschi[1], Nissim Hay[10], Peter Carmeliet[11,12], Thomas W. Chittenden[5], Anne Eichmann[1,13], Michael Potente[2] & Michael Simons[1,14]

GO Class	Accession Number	nGOSeq Term	List Hits	List Size	Pop Hits	Pop Size	Fisher's Exact	Gene Enrich	%Gene Enrich	Pvalue LogDiff	nGOseq Gene Enrich	GOseq Accession	GOSeq Term
BP	1900744	regulation of p38MAPK cascade	2	63	4	889	0.027	1.72	42.91	0.65	0.33	0007155	cell adhesion
BP	0060055	angiogenesis involved in wound healing	3	20	4	199	0.003	2.60	64.95	0.88	0.25	0001666	response to hypoxia
BP	0001935	endothelial cell proliferation	22	1127	72	7178	0.001	10.66	14.86	0.26	0.25	0044237	cellular metabolic process
BP	0043114	regulation of vascular permeability	2	85	4	868	0.050	1.61	40.21	0.68	0.54	0006629	lipid metabolic process
BP	0010573	vascular endothelial growth factor production	3	41	6	488	0.013	2.50	41.60	0.70	0.43	0033993	response to lipid
BP	0071604	transforming growth factor beta production	3	37	8	441	0.022	2.33	29.11	0.21	0.06	2000145	regulation of cell motility
BP	0006006	glucose metabolic process	19	576	73	3432	0.028	6.75	9.244	0.64	1.53	0044767	single-organism developmental process

Chittenden *et al.*, *Bioinformatics* 2012
Fang *et al.*, *Nature Communications* 2017
Yu *et al.*, *Nature* 2017

Blue = DNA Methylation
Red = mRNA
Orange = miRNA
Green = CNV
Pink = STV

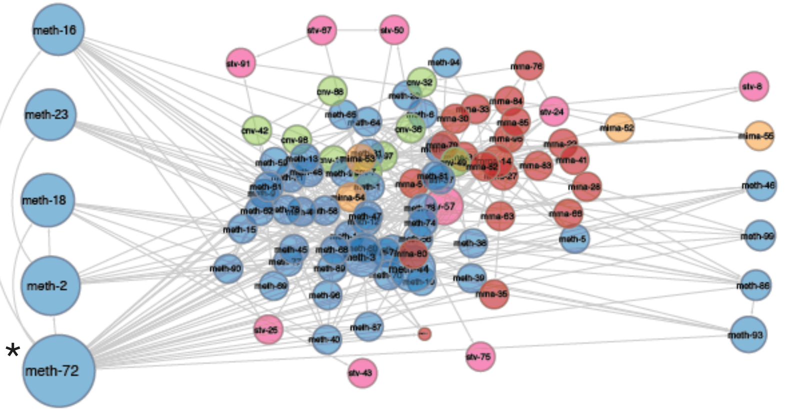

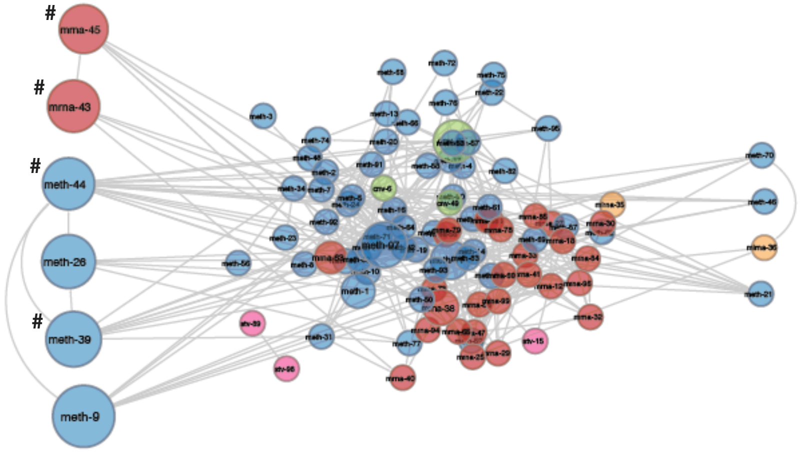

Bayesian Belief Networks

Purple Band = Degree NLP Network Connectivity
Black Band = Degree BNN Node Connectivity
Blue Band = Function Annotation
Red = BNN Driver Gene
Bold + Italic = Known Drug Target
*Driver Gene & Known Drug Target
#Driver Gene of Unknown Function

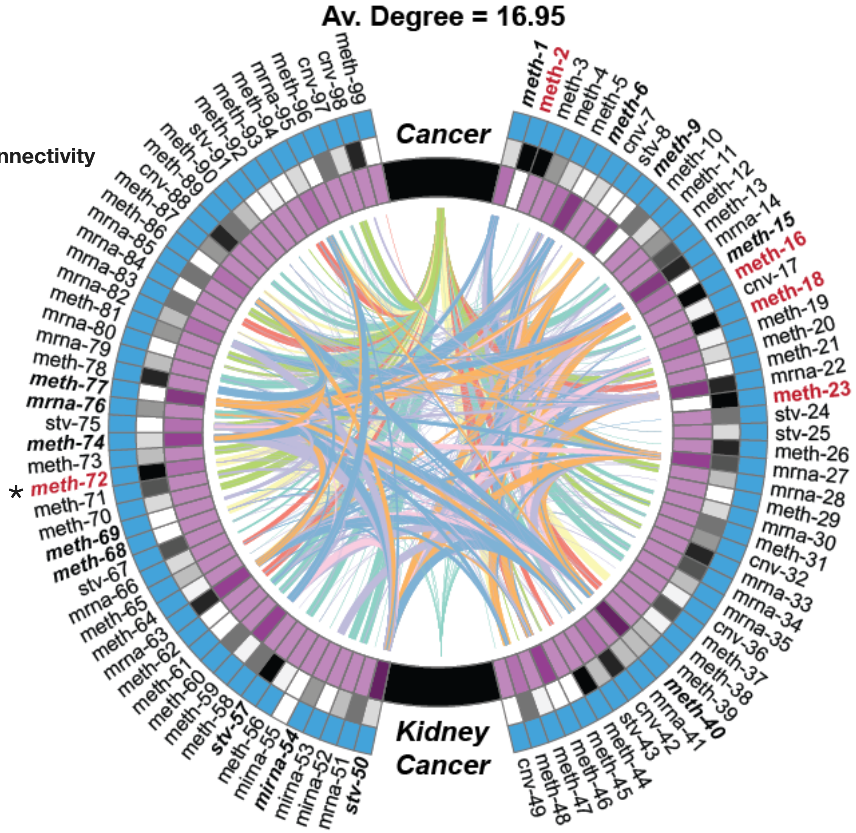

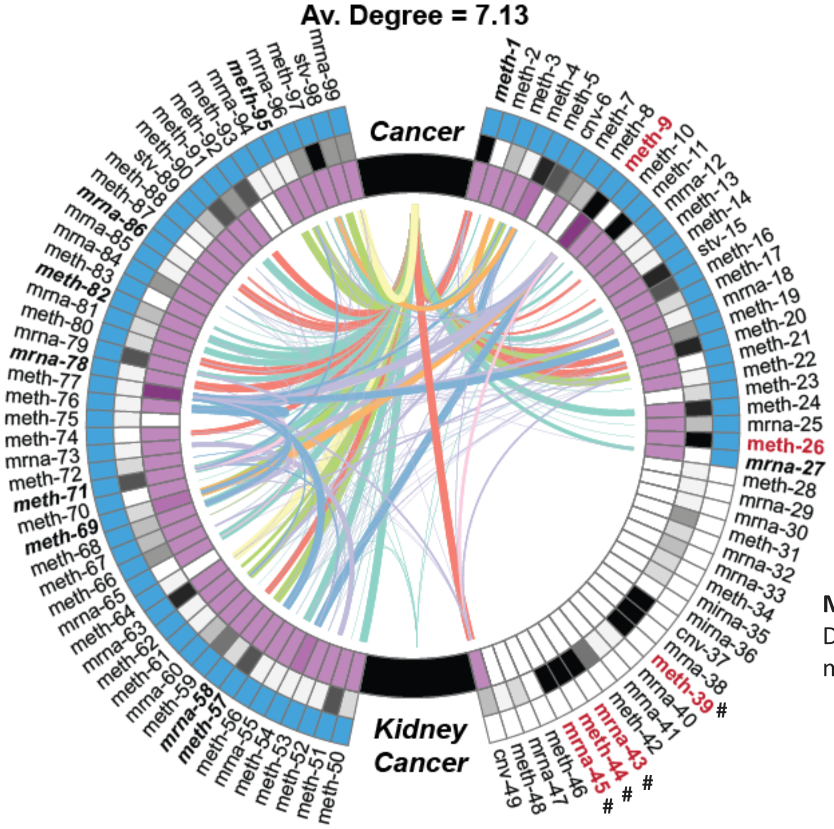

Natural Language Processing

nGOseq
DNA Methylation = 11
mRNA = 1
miRNA = 1
STV = 1

MEGENA
DNA Methylation = 6
mRNA = 4

nGOseq

MEGENA

WuXiNextCODE

Multinomial Classification of 22 TCGA Cancer Types with Greater than 99.6% Accuracy

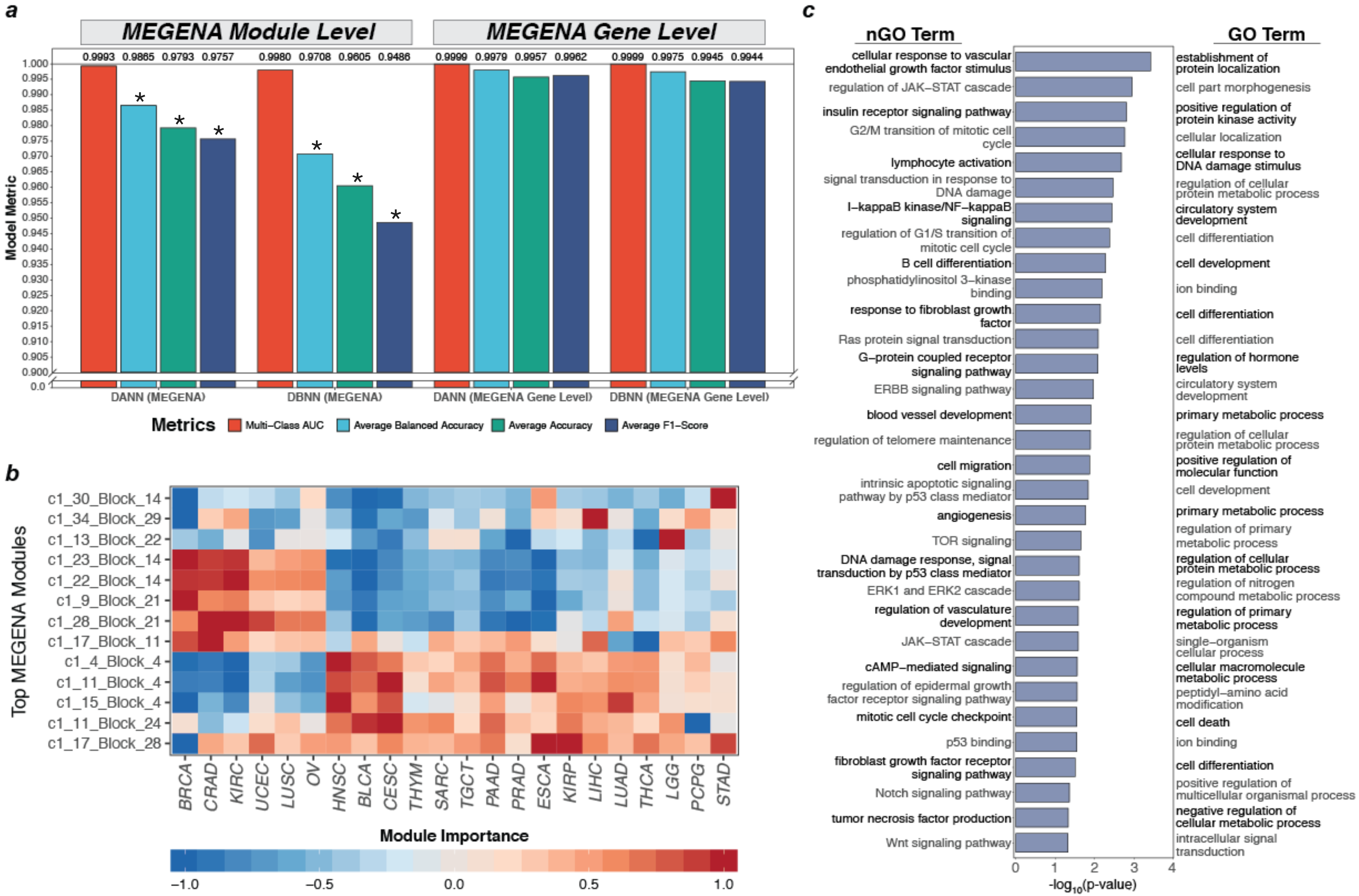

Multinomial Classification of 22 TGCA Cancer Types with Greater than 99.6% Accuracy

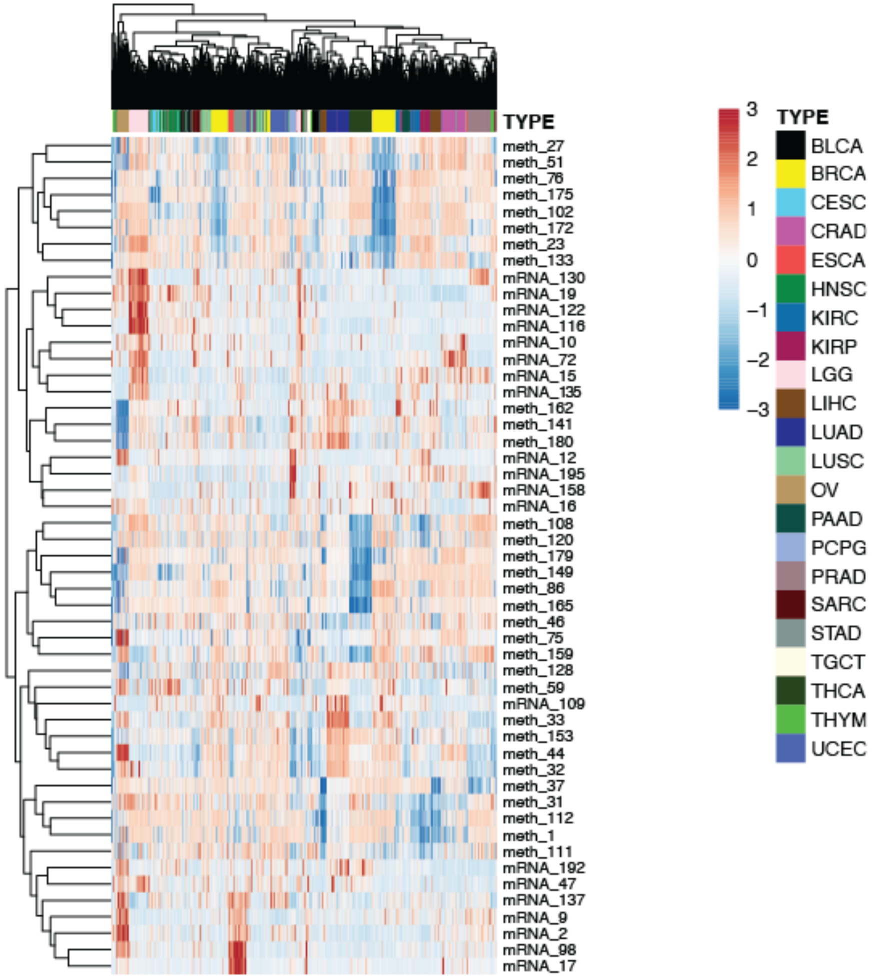

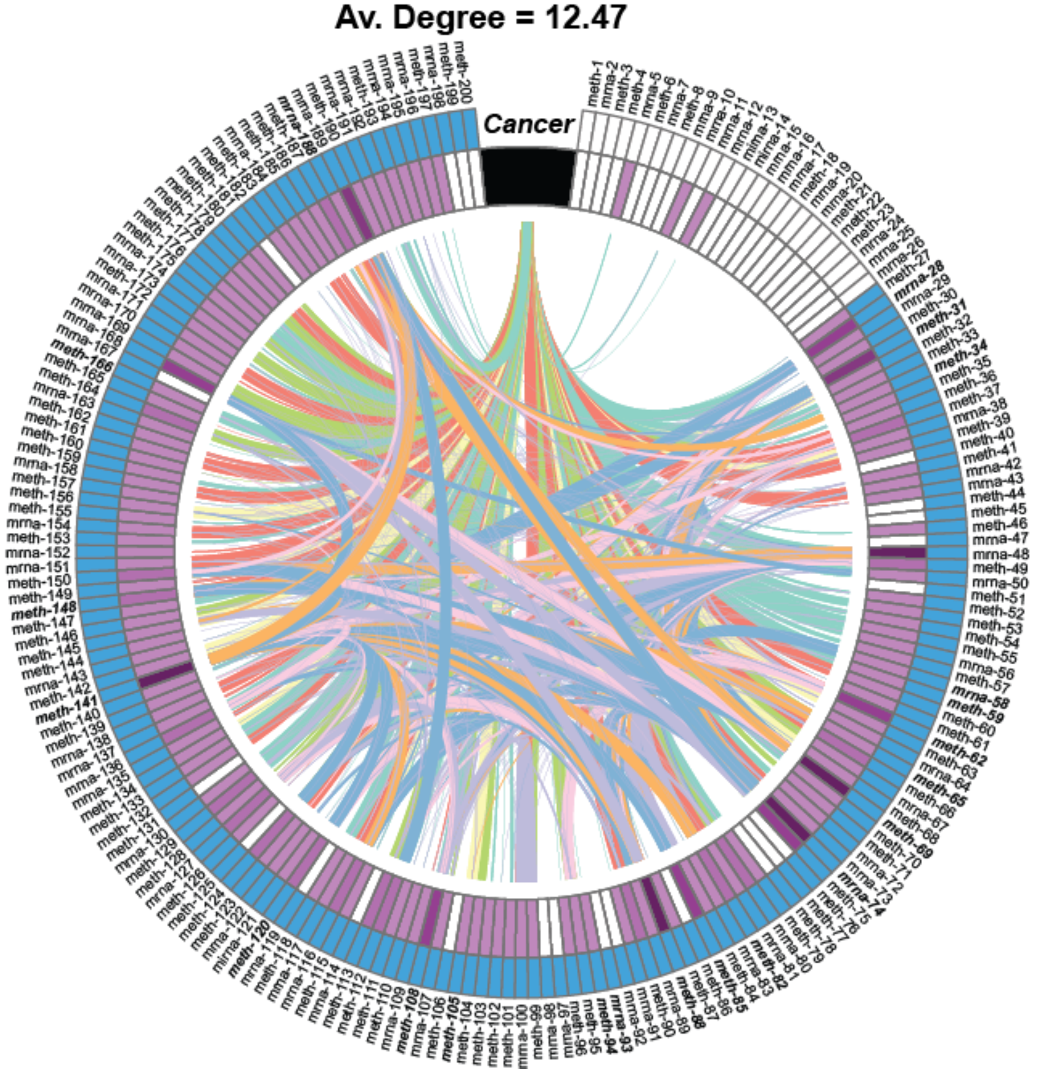

Natural Language Processing

Purple Band = Degree NLP Network Connectivity
Blue Band = Function Annotation
Bold + Italic = Known Drug Target (12 DNA Methylation; 4 mRNA)

Deep Learning, Machine Learning and Alzheimer Disease (ADNI)

Image Data

PET Scans (AV45 + FDG)

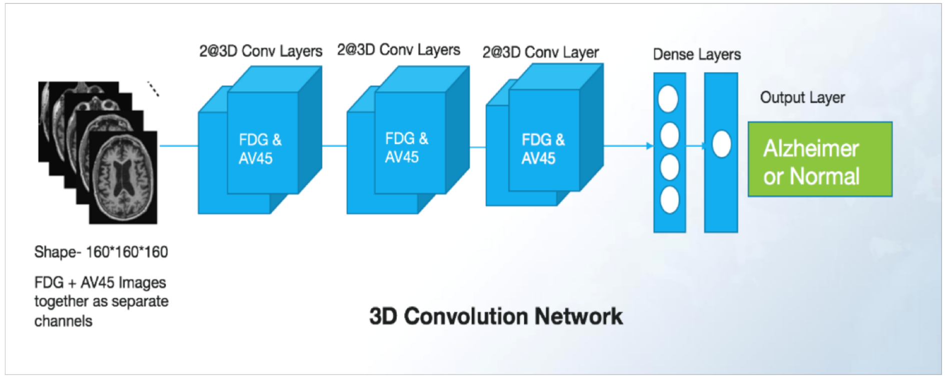

	Count
Samples	326
Alzheimer	144
Controls	182

DCNN (Test set)	
AUC	0.99
Accuracy	0.94

Molecular Signature

Integrated Datatypes: Methylation , Expression, Variant Data

	Count
Samples	152
Alzheimer	36 (29/7)
Controls	116 (93/23)

	LASSO (Test set)			
	MEGENA	nGOSeq	MEGENA	nGOSeq
	MetaGene	MetaGene	Gene	Gene
AUC	0.87	0.94	0.98	1
Accuracy	0.83	0.93	0.97	0.93

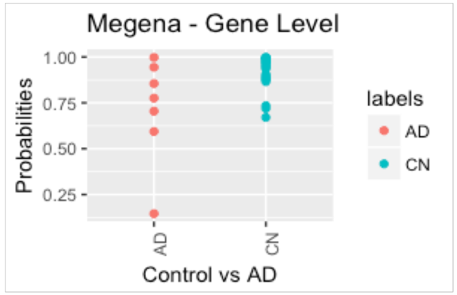

Non-zero Genes
Methylation: 31
Expression: 17
STV: 7

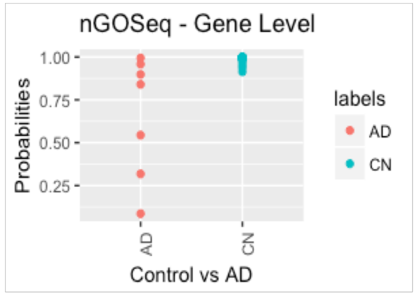

Non-zero Genes
Methylation: 29
Expression: 5
STV: 10

Deep Learning, Machine Learning and Alzheimer Disease (ADNI)

Molecular Signature

Single Datatypes: Methylation , Expression, Variant Data

	Count
Samples	152
Alzheimer	36 (29/7)
Controls	116 (93/23)

	Methylation Genes	Expression Genes	Variant Genes
AUC	0.93	0.77	0.80
Accuracy	0.90	0.76	0.77
AD Test Acc	0.57	0.54	0.54

No Feature Selection

	MEGENA Feature Selection		
	Methylation Genes	Expression Genes	Variant Genes
AUC	0.99	0.75	0.75
Accuracy	0.93	0.73	0.73
AD Test Acc	0.86	0.64	0.64

	nGOSeq Feature Selection		
	Methylation Genes	Expression Genes	Variant Genes
AUC	0.98	0.81	0.75
Accuracy	0.93	0.73	0.73
AD Test Acc	0.71	0.64	0.58

Blue = DNA Methylation
Red = mRNA
Pink = STV

#Same Gene

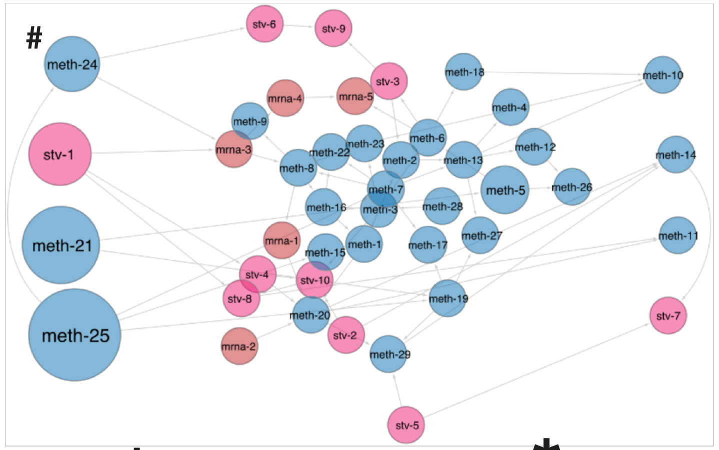

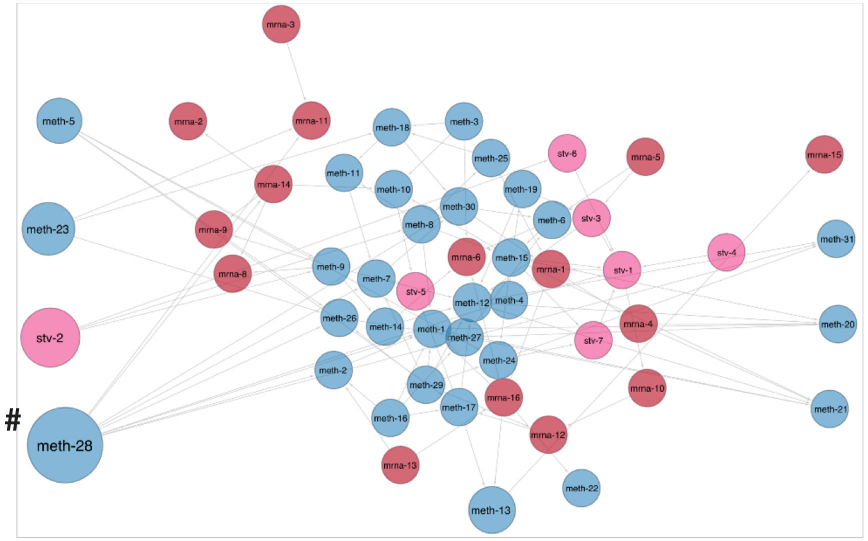

Bayesian Belief Networks

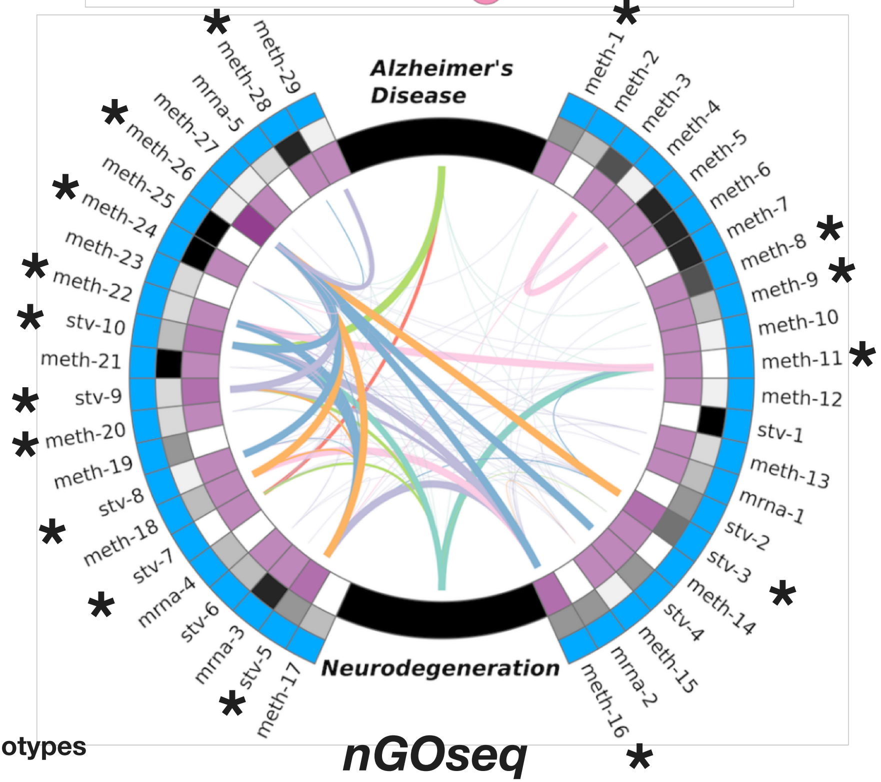

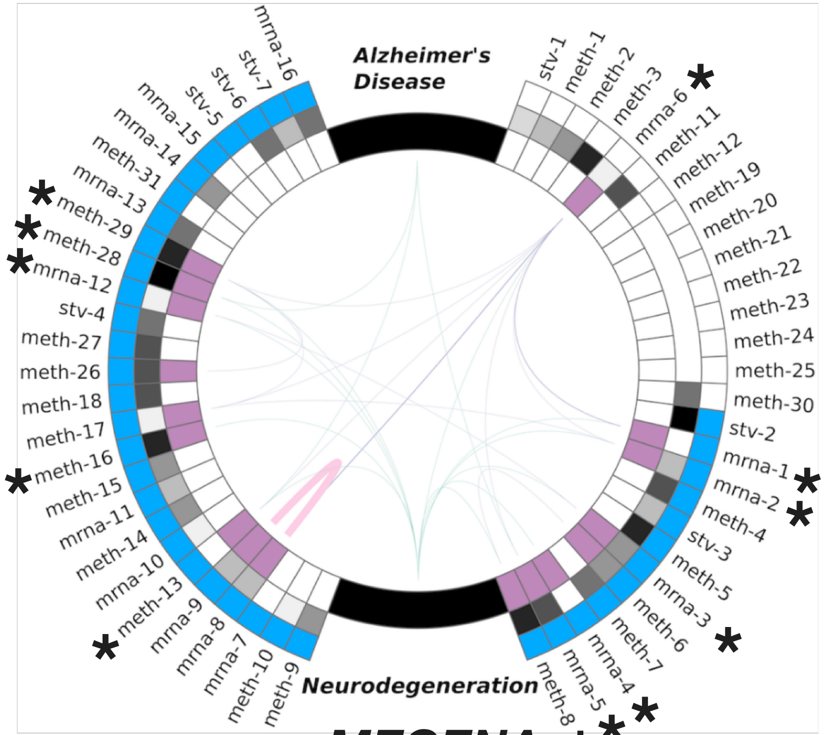

Natural Language Processing

*Implicated in Phenotypes

nGOseq

Av. Degree = 12.00

MEGENA

Av. Degree = 4.58

WuXiNextCODE

Deep Learning, Machine Learning and Alzheimer Disease (RosMap)

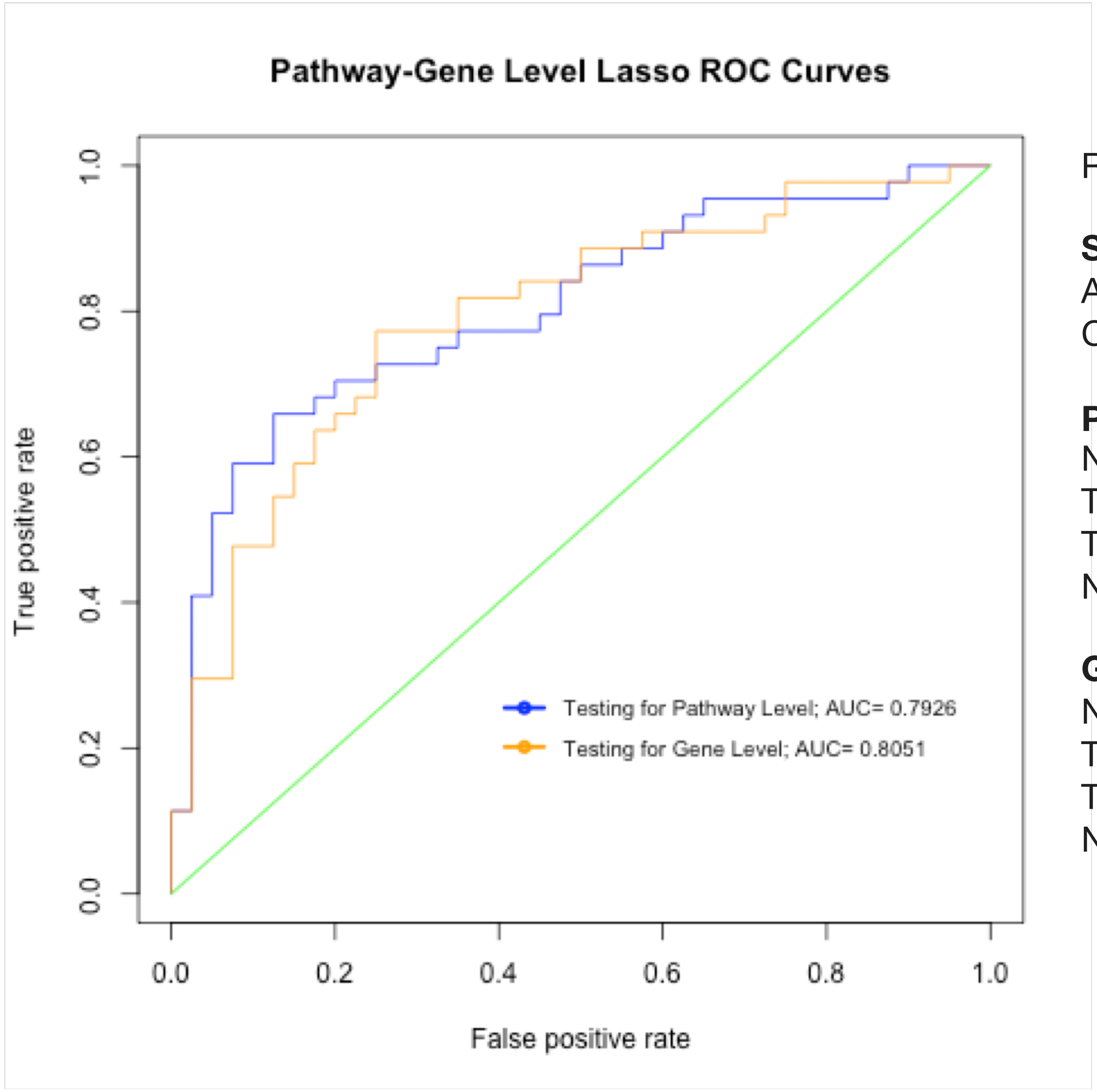

RNA extracted from dorsolateral prefrontal cortex of 724 subjects

Sample set:
AD: 222 [Train: 178, Test: 44]
CN: 201 [Train: 161, Test: 40]

Pathway Level Analysis:
Number of Pathways: 3340
Test Accuracy: 72.61
Test AUC: 79.26
Number of Non-Zero Pathways: 76

Gene Level Analysis:
Number of Genes: 342 Genes from 76 Non-zero Pathways
Test Accuracy: 72.61
Test AUC: 80.51
Number of Non-Zero Genes: 45

WuXiNextCODE

Deep Learning for Chemical Reactions

Modeling Chemical Data

DL models based on different representations of molecules:

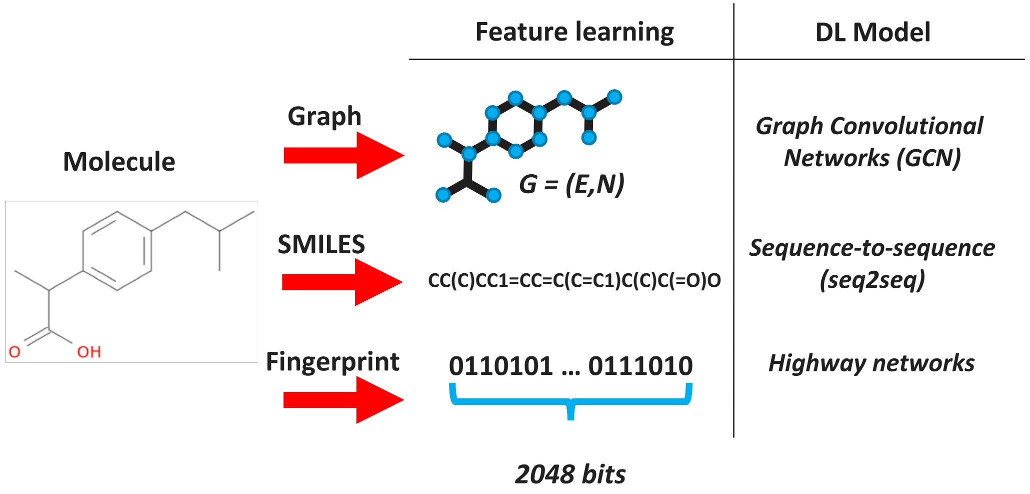

Retrosynthesis

Learning how molecules are produced using chemical reaction datasets (~1.1 M chemical reactions from U.S. patents)

	Count
Product molecules	431485
Chemical reactions for classification	462

Multinomial classification with Highway networks (20% - Test set)	
Accuracy	0.79 (0.12)*

Multinomial classification with Multiscale approach (20% - Test set)	
Accuracy	0.90 (0.08)*

*s.d. in parentheses

Taking stereochemistry into account

Learning about molecular 3D shape for chemical reaction prediction

Atoms can be arranged differently for same molecule:

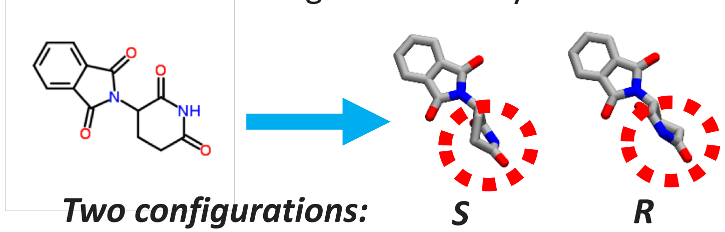

	Count
Molecules with single chiral center	2762

Binomial classification based on chirality (20% - Test set)	
Accuracy	0.89

Modeling Human Breast Cancers
Quantum Machine Learning

Classical HCL

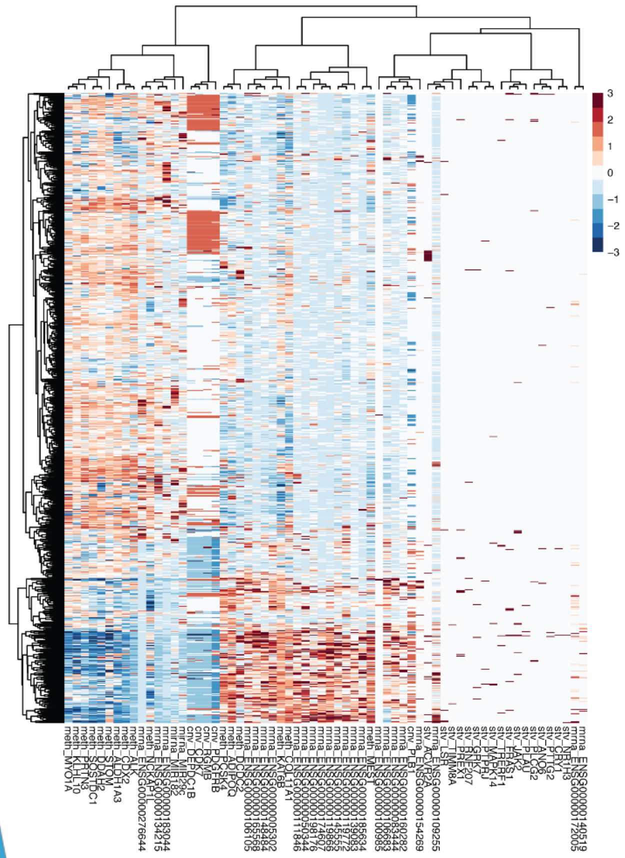

Estrogen Receptor Status	
Tumor Samples	959
ER Negative	740
ER Positive	219
Train	768
Test	191

	Performance	
Algorithm	HCL	qHCL
Clustering (genes)	64	64
Clustering (sec)*	0.02	10078.30 (2h 48m)
Cluster Number	8	9
LASSO Classification Accuracy	0.9215	0.9267
LASSO ROC AUC	0.945	0.944
DANN Classification Accuracy	0.9267	0.9267
DANN ROC AUC	0.943	0.944

*Quantum and classical trees are 88% concordant based on the standard Robinson–Foulds metric

*qHCL - Durr-Hoyer method based on a modified Grover's search algorithm with Euclidean distance and Ward linkage

*qHCL ran on a IBM quantum simulator using 19 qubits

quantum HCL

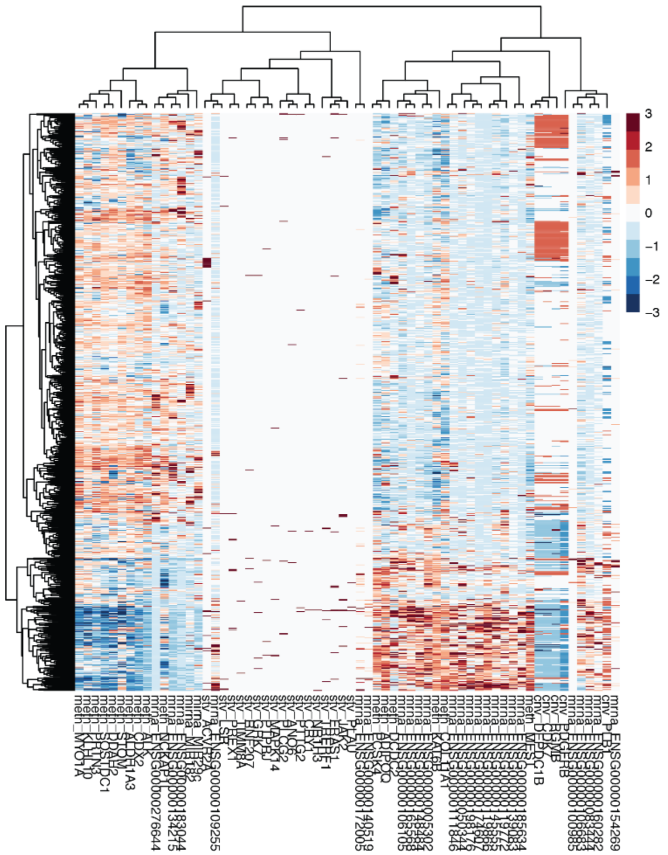

WUXI NEXTCODE ANALYSIS PLATFORM

Clinical interpretation and research in **one, scalable platform built for the genome from the ground up**

GOR (Genomically Ordered Relational) Database Infrastructure

- For efficient storage and queries for whole genome and whole exome data using the tools listed below

Clinical Sequence Analyzer (CSA)

- Clinical geneticist-friendly tools for germline analysis of large or small families
- Automatic gene carrier analysis for confirmation
- Generate candidate genes from a standard list or with phenotype tools and stratify by variant annotations

Sequence Miner (SM)

- Advanced tool for case-control disease gene discovery or responder non-responder companion diagnostic discovery
- Additional algorithms for covariate adjustment and pathway enrichment
- Perform phenotype scans and carrier analysis

Tumor Mutation Analyzer (TMA)

- Somatic variant analysis for defining tumor-specific variations and oncology annotations including actionable databases

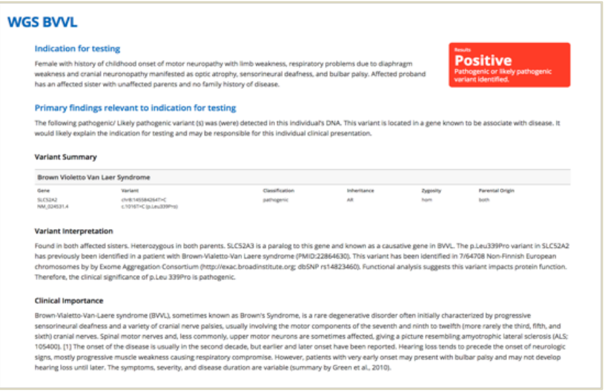

WGS BVVL

Indication for testing

Female with history of childhood onset of motor neuropathy with limb weakness, respiratory problems due to diaphragm weakness and cranial neuronopathy manifested as optic atrophy, sensorineural deafness, and bulbar palsy. Affected proband has an affected sister with unaffected parents and no family history of disease.

Results
Positive
Pathogenic or likely pathogenic variant identified.

Primary findings relevant to indication for testing

The following pathogenic/ Likely pathogenic variant (s) was (were) detected in this individual's DNA. This variant is located in a gene known to be associate with disease. It would likely explain the indication for testing and may be responsible for this individual clinical presentation.

Variant Summary

Brown Violetto Van Laer Syndrome

Gene	Variant	Classification	Inheritance	Zygosity	Parental Origin
SLC52A2 NM_024531.4	chr8:145584264T>C c.1016T>C (p.Leu339Pro)	pathogenic	AR	hom	both

Variant Interpretation

Found in both affected sisters. Heterozygous in both parents. SLC52A3 is a paralog to this gene and known as a causative gene in BVVL. The p.Leu339Pro variant in SLC52A2 has previously been identified in a patient with Brown-Vialetto-Van Laere syndrome (PMID:22864630). This variant has been identified in 7/64708 Non-Finnish European chromosomes by by Exome Aggregation Consortium (http://exac.broadinstitute.org; dbSNP rs14823460). Functional analysis suggests this variant impacts protein function. Therefore, the clinical significance of p.Leu 339Pro is pathogenic.

Clinical Importance

Brown-Vialetto-Van-Laere syndrome (BVVL), sometimes known as Brown's Syndrome, is a rare degenerative disorder often initially characterized by progressive sensorineural deafness and a variety of cranial nerve palsies, usually involving the motor components of the seventh and ninth to twelfth (more rarely the third, fifth, and sixth) cranial nerves. Spinal motor nerves and, less commonly, upper motor neurons are sometimes affected, giving a picture resembling amyotrophic lateral sclerosis (ALS; 105400). [1] The onset of the disease is usually in the second decade, but earlier and later onset have been reported. Hearing loss tends to precede the onset of neurologic signs, mostly progressive muscle weakness causing respiratory compromise. However, patients with very early onset may present with bulbar palsy and may not develop hearing loss until later. The symptoms, severity, and disease duration are variable (summary by Green et al., 2010).

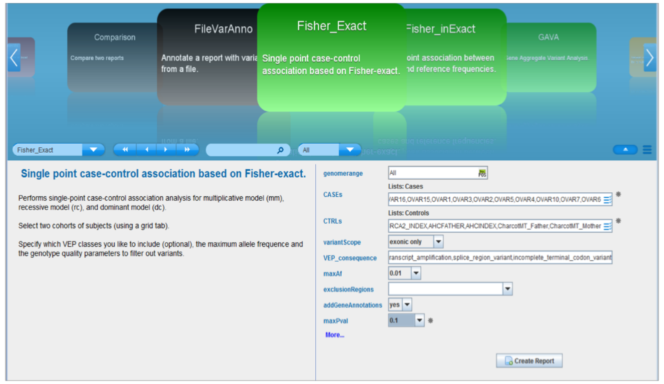
Comparison
Compare two reports
FileVarAnno
Annotate a report with varia from a file.
Fisher_Exact
Single point case-control association based on Fisher-exact.
Fisher_inExact
oint association between nd reference frequencies.
GAVA
Gene Aggregate Variant Analysis.
Fisher_Exact
All
More...
Create Report

Single point case-control association based on Fisher-exact.

Performs single-point case-control association analysis for multiplicative model (mm), recessive model (rc), and dominant model (dc).

Select two cohorts of subjects (using a grid tab).

Specify which VEP classes you like to include (optional), the maximum allele frequence and the genotype quality parameters to filter out variants.

genomerange: All

CASEs: Lists: Cases /AR16,OVAR15,OVAR1,OVAR3,OVAR2,OVAR5,OVAR4,OVAR10,OVAR7,OVAR6

CTRLs: Lists: Controls RCA2_INDEX,AHCFATHER,AHCINDEX,CharcotMT_Father,CharcotMT_Mother

variantScope: exonic only

VEP_consequence: ranscript_amplification,splice_region_variant,incomplete_terminal_codon_variant

maxAf: 0.01

exclusionRegions:

addGeneAnnotations: yes

maxPval: 0.1

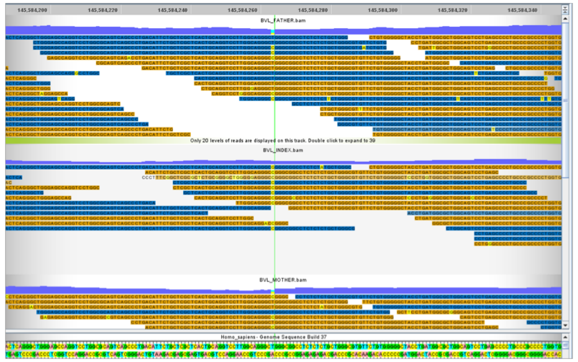
145,584,200
145,584,220
145,584,240
145,584,260
145,584,280
145,584,300
145,584,320
145,584,340
BVL_FATHER.bam
Only 20 levels of reads are displayed on this track. Double click to expand to 39
BVL_INDEX.bam
BVL_MOTHER.bam
Homo_sapiens - Genome Sequence Build 37